SUSTAINED MONITORING OF THE SOUTHERN OCEAN AT DRAKE PASSAGE: PAST ACHIEVEMENTS AND FUTURE PRIORITIES

Michael P. Meredith,[1] Philip L. Woodworth,[2] Teresa K. Chereskin,[3] David P. Marshall,[4] Lesley C. Allison,[5] Grant R. Bigg,[6] Kathy Donohue,[7] Karen J. Heywood,[8] Chris W. Hughes,[2] Angela Hibbert,[9] Andrew McC. Hogg,[10] Helen L. Johnson,[11] Loïc Jullion,[12] Brian A. King,[12] Harry Leach,[9] Yueng-Djern Lenn,[13] Miguel A. Morales Maqueda,[2] David R. Munday,[4] Alberto C. Naveira Garabato,[12] Christine Provost,[14] Jean-Baptiste Sallée,[1] and Janet Sprintall[3]

[1] Drake Passage is the narrowest constriction of the Antarctic Circumpolar Current (ACC) in the Southern Ocean, with implications for global ocean circulation and climate. We review the long-term sustained monitoring programs that have been conducted at Drake Passage, dating back to the early part of the twentieth century. Attention is drawn to numerous breakthroughs that have been made from these programs, including (1) the first determinations of the complex ACC structure and early quantifications of its transport; (2) realization that the ACC transport is remarkably steady over interannual and longer periods, and a growing understanding of the processes responsible for this; (3) recognition of the role of coupled climate modes in dictating the horizontal transport and the role of anthropogenic processes in this; and (4) understanding of mechanisms driving changes in both the upper and lower limbs of the Southern Ocean overturning circulation and their impacts. It is argued that monitoring of this passage remains a high priority for oceanographic and climate research but that strategic improvements could be made concerning how this is conducted. In particular, long-term programs should concentrate on delivering quantifications of key variables of direct relevance to large-scale environmental issues: In this context, the time-varying overturning circulation is, if anything, even more compelling a target than the ACC flow. Further, there is a need for better international resource sharing and improved spatiotemporal coordination of the measurements. If achieved, the improvements in understanding of important climatic issues deriving from Drake Passage monitoring can be sustained into the future.

1. THE GLOBAL SIGNIFICANCE OF DRAKE PASSAGE AND THE NEED FOR SUSTAINED OBSERVATIONS

1.1. Drake Passage, Global Circulation, and Climate

[2] Owing to its unique geography, the Southern Ocean exerts a profound influence on global ocean circulation. In particular, the presence of zonally unblocked latitudes in the Southern Ocean permits the flow of the only current to circumnavigate the globe, namely, the Antarctic Circumpolar Current (ACC) (Figure 1). This is the largest current system in the world, and it plays a key role in connecting the three major ocean basins (Figure 2), allowing an interbasin exchange of heat, salt, carbon, and other chemical and biological properties. Associated with the strong eastward flow of the ACC, density surfaces tilt strongly upward toward the south in the Southern Ocean, exposing dense layers of the ocean to interaction with the atmosphere and cryosphere. This acts to

[1]British Antarctic Survey, Cambridge, UK.
[2]National Oceanography Centre, Liverpool, UK.
[3]Scripps Institution of Oceanography, La Jolla, California, USA.
[4]Atmospheric, Oceanic and Planetary Physics, University of Oxford, Oxford, UK.
[5]Department of Meteorology, University of Reading, Reading, UK.
[6]Department of Geography, University of Sheffield, Sheffield, UK.
[7]Graduate School of Oceanography, University of Rhode Island, Kingston, Rhode Island, USA.
[8]School of Environmental Sciences, University of East Anglia, Norwich, UK.
[9]Department of Earth and Ocean Sciences, University of Liverpool, Liverpool, UK.
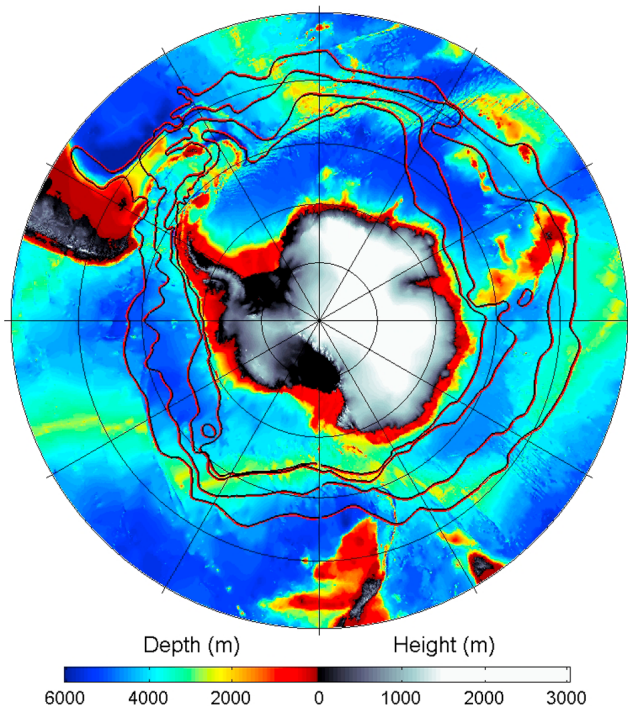[10]Research School of Earth Sciences, Australian National University, Canberra, ACT, Australia.
[11]Department of Earth Sciences, University of Oxford, Oxford, UK.
[12]National Oceanography Centre, Southampton, UK.
[13]School of Ocean Sciences, Bangor University, Bangor, UK.
[14]LOCEAN, Université Pierre et Marie Curie, Paris, France.

Figure 1. Bathymetry and topography of the Southern Ocean and Antarctica. Marked schematically is the Antarctic Circumpolar Current, denoted by the approximate positions of its main frontal features [*Orsi et al.*, 1995]. Drake Passage, between South America and the Antarctic Peninsula, is the most significant choke point for the ACC as it circumnavigates Antarctica.

transfer water between density classes, and leads to the existence of a vigorous overturning circulation in the Southern Ocean. This can be viewed as two counterrotating upper and lower cells (Figure 2) [*Lumpkin and Speer*, 2007]. Because of its strong three-dimensional circulation, the ACC is a key component of the global climate system [*Rintoul et al.*, 2001].

[3] Lying between the South American and Antarctic continents, Drake Passage (Figure 3, top left) is the region of narrowest constriction of the ACC and, as such, exerts a strong constraint on both its path and strength. The passage has a width of roughly 800 km, although the submerged barrier blocking circumpolar contours at depth is located further east, around the edges of the Scotia Sea. The precise timing of the opening of Drake Passage remains controversial. *Livermore et al.* [2005] date the opening of a shallow connection during the Early Eocene (~50 Ma) with a deep water connection developing around the Eocene-Oligocene boundary (34–30 Ma), on the basis of analysis of marine geophysical data. These results are broadly consistent with analysis of neodymium isotope ratios in the Atlantic sector that indicate an influx of shallow Pacific water around 41 Ma [*Scher and Martin*, 2006], although other studies date the opening somewhat later [*Barker*, 2001]. Associated with the uncertainty concerning the timing of the opening of Drake Passage, the initiation of the ACC remains similarly uncertain [*Barker et al.*, 2007]. Nevertheless, the hypothesis that Drake

Passage opened during the Eocene, allowing the onset of a form of the ACC and development of Antarctica's climatic isolation, is consistent with the gradual decline in global temperature from ~50 Ma, followed by abrupt cooling and the onset of glaciation at 33–34 Ma [*Zachos et al.*, 2001].

[4] Dynamically, the pivotal importance of Drake Passage is due to the absence of zonal pressure gradients within the ocean there. At other (blocked) latitudes, the zonal wind stress at the surface can be balanced by zonal pressure gradients within the upper few hundred meters: Any directly wind-forced transport at the surface (i.e., equatorward Ekman transport) can then be opposed by poleward geostrophic transport, leading to shallow overturning Ekman cells. However, in the absence of continental barriers at the latitudes of Drake Passage, the compensating poleward geostrophic transport can only occur at depth, where submerged topography is able to support a zonal pressure gradient [*Munk and Palmén*, 1951]. This leads to a wind-driven overturning "Deacon cell" that extends much deeper. In concert with surface thermal forcing that maintains a surface buoyancy gradient, this Deacon cell mechanically pumps down warm, buoyant water to the north of the ACC, leading to the establishment of a global pycnocline [*Gnanadesikan and Hallberg*, 2000; *Karsten et al.*, 2002; *Vallis*, 2000]. Consistent with this conceptual picture is the result that Southern Ocean wind forcing is the dominant mechanical energy source for the global ocean [*Wunsch and Ferrari*, 2004].

[5] The steepening of the isopycnals by the continuous input of momentum from the winds is ultimately arrested by baroclinic instability, the wind-driven Deacon Cell being opposed by an eddy-driven bolus overturning cell [*Gent et al.*, 1995]. In early numerical simulations, this compensation between wind- and eddy-driven overturning cells was nearly exact, resulting in virtually no residual overturning
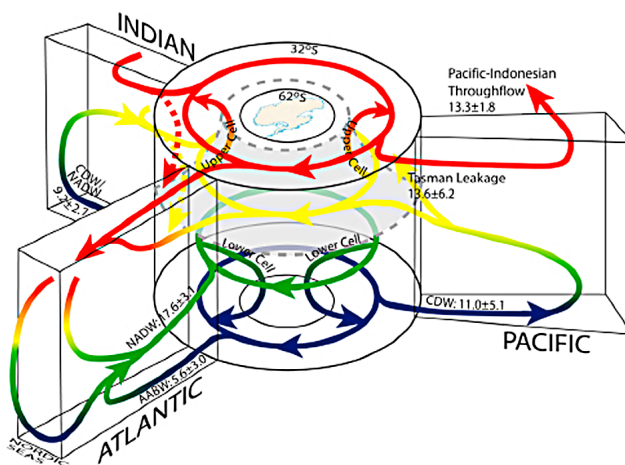
Figure 2. Schematic diagram of the global overturning circulation (reproduced from *Lumpkin and Speer* [2007]). The arrows indicate the net overturning circulation, integrated across each ocean basin, with the numbers indicating the volume transports of each water mass (Sv). This illustrates the critical role of the Southern Ocean in connecting the overturning cells in each of the basins to the north.
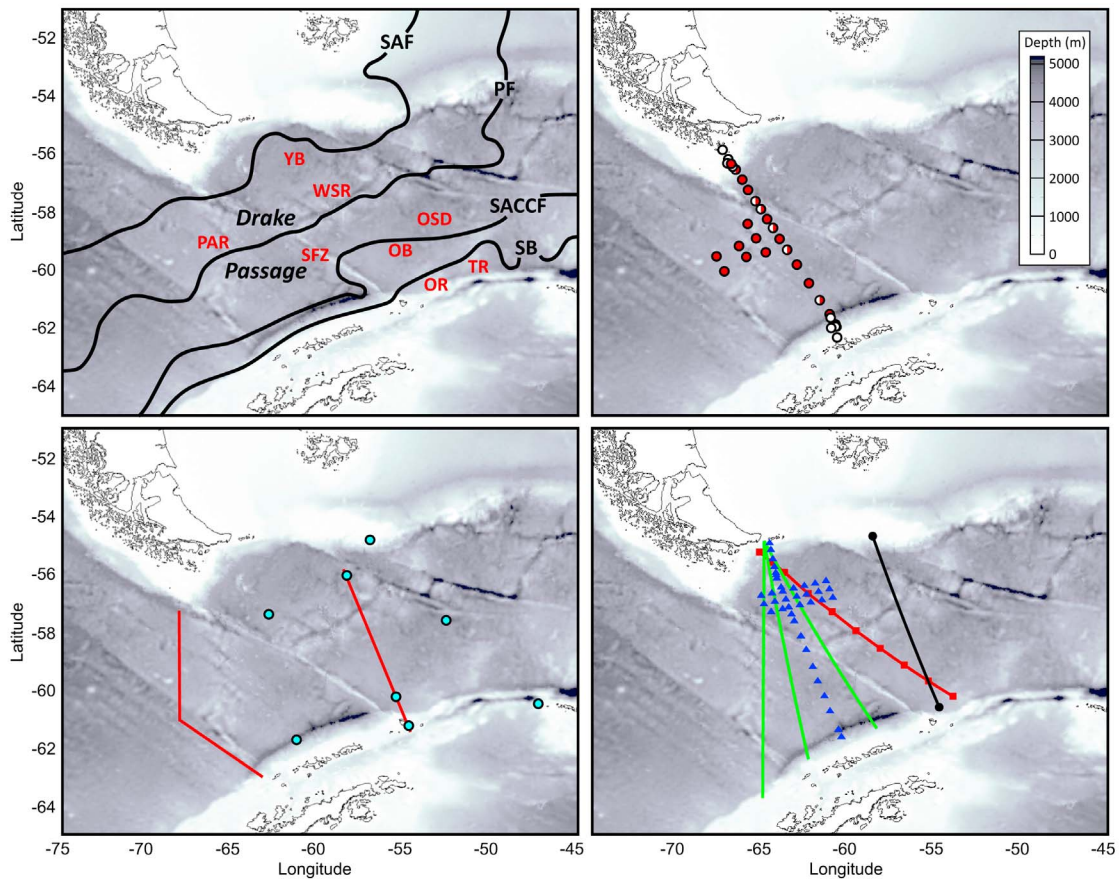
Figure 3. (top left) Bathymetry of Drake Passage and a schematic depiction of the main frontal features, namely, the SAF, Subantarctic Front; PF, Polar Front; SACCF, Southern ACC Front; SB, Southern Boundary. Various topographic features are also marked: YB, Yaghan Basin; OB, Ona Basin; PAR, Phoenix Antarctic Ridge, SFZ, Shackleton Fraction Zone; WSR, West Scotia Ridge; OSD, Ona Seafloor Depression. (top right) The Drake Passage monitoring system during the ISOS era: red circles denote current meter moorings, white circles denote bottom pressure recorders (BPRs), and occluded symbols are current meter moorings with incomplete data return. (bottom left) The Drake Passage monitoring system during WOCE: blue circles denote BPRs and red lines denote WOCE repeat hydrography lines SR1 (western line) and SR1b (eastern line). (bottom right) The contemporary monitoring system in Drake Passage: green lines denote repeat XBT-ADCP lines, blue triangles denote the CPIES array, red squares denote the DRAKE current meter array, black line denotes the SR1b repeat hydrography line, and black circles denote BPRs.

circulation [see also *Danabasoglu et al.*, 1994; *Döös and Webb*, 1994]. More generally, in thermodynamic equilibrium, the strength of the residual circulation is related to the surface buoyancy forcing [*Marshall*, 1997], with surface wind and buoyancy forcing and interior eddy fluxes combining to set both the stratification of the ACC, its volume transport through Drake Passage and the residual overturning circulation [*Marshall and Radko*, 2003]. These ideas have been extended and applied to observed air-sea fluxes to infer the residual overturning [*Karsten and Marshall*, 2002; *Olbers and Visbeck*, 2005; *Speer et al.*, 2000]. The schematic of the overturning circulation in the major ocean basins shown in Figure 2 emphasizes the key role of these Southern Ocean processes in the formation and transformation of globally important water masses [*Lumpkin and Speer*, 2007].

[6] The preceding discussion has emphasized the role of local forcing over the Southern Ocean in setting the ACC

transport through Drake Passage and the residual overturning circulation. However, it is important to note also that the ACC is intimately coupled with the global ocean circulation and stratification, as elegantly articulated in the conceptual model of *Gnanadesikan* [1999] for the global pycnocline, and its application to the ACC [*Gnanadesikan and Hallberg*, 2000]. This explains, for example, how Southern Ocean winds can influence the strength of the North Atlantic meridional overturning circulation (the "Drake Passage effect" [e.g., *Toggweiler and Samuels*, 1995]) and, conversely, how the rate of North Atlantic Deep Water (NADW) formation can influence the ACC transport through Drake Passage [*Fučkar and Vallis*, 2007]. Likewise, *Munday et al.* [2011] have shown that diapycnal mixing in the northern basins can significantly affect the ACC transport through Drake Passage. Such models have also been useful in clarifying that most of the wind forcing

of the ACC occurs north of Drake Passage, with the most appropriate measure of the "Southern Ocean wind stress" being an integral over the circumpolar streamlines [*Allison et al.*, 2010].

[7] Via its strong overturning circulation, the Southern Ocean also has a major influence on the ocean carbon cycle. Changes in the overturning across the ACC impact the air-sea carbon flux and biological productivity, and are widely believed to be important for explaining the large glacial-interglacial changes in atmospheric CO_2 [e.g., *Watson and Naveira Garabato*, 2006]. Outcropping isopycnals in the Southern Ocean also provide an important pathway for the subduction of anthropogenic CO_2 into the ocean interior [*Caldeira and Duffy*, 2000; *Sabine et al.*, 2004] via the upper cell. The climate system is therefore sensitive to changes in the residual overturning circulation with the potential for feedbacks onto the Southern Ocean sink of anthropogenic CO_2 [*Mignone et al.*, 2006].

1.2. Specific Rationale for Sustained Observations in Drake Passage

[8] The pivotal role of the ACC in global climate makes it a priority for any global network of sustained climate observations. Logistically, by far the most practical location to monitor the ACC is across Drake Passage. First, this is the narrowest constriction across the Southern Ocean, thus allowing the full meridional extent of the ACC to be covered with the minimal possible effort. Second, with continental landmasses to the north and south, Drake Passage is the only place across which one can unambiguously monitor the ACC without the complicating influence of subpolar and subtropical flows on its flanks. Third, Drake Passage lies immediately north of the most inhabited part of Antarctica, thus it is the region of the Southern Ocean most frequented by supply vessels, presenting greatest opportunities for the synergistic use of ship time.

[9] As discussed above and illustrated in Figure 2, Drake Passage represents a crossroads for the global overturning circulation. It is of specific interest because it lies along the "cold water path" for overturning waters returning to the Atlantic, in contrast to the "warm water path" via the Indonesian Throughflow and Agulhas leakage [*Gordon*, 1986]. As one of the most critical choke points in the global ocean, Drake Passage is a natural point at which to attempt quantification of the time-varying fluxes of heat, freshwater and other tracers, in order to provide strong constraints on water mass budgets and circulation patterns within each of the major basins.

[10] Drake Passage is fortuitously situated for monitoring changes in the water masses that occupy both the upper and lower limbs of the overturning circulation in the Atlantic. For example, Subantarctic Mode Water (SAMW), formed by deepening of the winter mixed layer on the equatorward flank of the ACC, has a pronounced source in the southeast Pacific [*Aoki et al.*, 2007], from where it flows through Drake Passage into the Atlantic. Lying beneath the SAMW is Antarctic Intermediate Water (AAIW), which forms from upwelled Circumpolar Deep Water (CDW) that becomes

Antarctic Surface Water (AASW) and subducts at the Polar Front. The AAIW found in Drake Passage originates in the winter mixed layer of the Bellingshausen Sea [*Naveira Garabato et al.*, 2009]. The eastern part of Drake Passage is also close to the outflow of the Weddell Sea Deep Water (WSDW) that forms at the periphery of Antarctica in the southern and western Weddell Sea. Upon entering the Scotia Sea, WSDW can flow westward toward Drake Passage, or northeastward toward the Georgia and Argentine basins [*Naveira Garabato et al.*, 2002a]. Since WSDW ultimately constitutes the densest component of the Antarctic Bottom Water (AABW) in the Atlantic Meridional Overturning Circulation, observations across Drake Passage can yield information on the lower limb of this overturning, and constitute a powerful complement to time series generated from within the ice-infested subpolar gyre [e.g., *Gordon et al.*, 2010; *Meredith et al.*, 2011].

[11] Each of the water masses in Drake Passage has been seen to be changing significantly in recent times [*Bindoff et al.*, 2007; *Gille*, 2008; *Jullion et al.*, 2010; *Naveira Garabato et al.*, 2009]. There is much interest in understanding to what extent these changes are of anthropogenic origin, as opposed to representing natural variability. A prerequisite for this is to sample the changes with spatial consistency and with sufficient temporal resolution to avoid aliasing problems and to permit correct determination of the time scale of the variability; only in this way can proper attribution even be attempted. This further underlines the importance of sustained observations, and will be discussed in more detail section 3.

[12] For all of the reasons described above, the Drake Passage is now the most measured stretch of water in the Southern Ocean, and historically one of the most heavily monitored intercontinental straits in the global ocean. Consequently, any changes in Southern Ocean properties or fluxes are most likely to be recognized and interpreted correctly here.

1.3. Aims and Structure of the Paper

[13] This paper aims to provide a review of sustained observations at Drake Passage since the very early days of Southern Ocean science, a summary of the most important results that have been obtained to date, and an assessment of current activities, to guide what might be done in the future. Section 2 reviews the early attempts to monitor the Southern Ocean at Drake Passage, including the landmark International Southern Ocean Studies (ISOS) experiment. Section 3 describes the initiatives that were undertaken during the World Ocean Circulation Experiment (WOCE), which was the largest ever physical oceanographic program, and which had a specific focus on the Southern Ocean. Many of these monitoring projects have continued up to the present day, so section 3 brings some of the WOCE-era findings up to date. Section 4 outlines some of the newer initiatives that have been instigated at Drake Passage since the end of WOCE, including some very recent additions to the monitoring effort that are just beginning to produce important new results. Section 5 summarizes some of the key findings

obtained from these programs, and considers which aspects of Drake Passage sustained observations should be maintained into the future, and why, as well as discussing where such monitoring efforts might be strategically improved.

2. EARLY DRAKE PASSAGE TRANSPORT MEASUREMENTS

[14] Prior to the ISOS program, which commenced in the mid-1970s, there was little by way of sustained observations of the ocean in Drake Passage. Most of the information that was accumulated during the pre-ISOS period was obtained from temporally sparse hydrographic sections and is reviewed by *Peterson* [1988a]. The main scientific target for these investigations was to determine the total volume transport through the passage.

[15] The first such hydrographic-section-based estimate of ACC transport was given by *Clowes* [1933], who used data from the *Discovery* expeditions during 1929–1930 to derive a transport relative to 3500 m of 110 Sv. The data used for this estimate were collected using techniques from an early era of oceanography, and much about the spatial structure of the ACC was unknown, however this value is strikingly similar to modern values for the transport through Drake Passage. Significantly, *Clowes* [1933] made an early realization that the eastward flow of the ACC at Drake Passage extends to great depths.

[16] In retrospect, this was a very good start, although the transport of the ACC at Drake Passage subsequently became the topic of considerable uncertainty. Purely on the basis of hydrographic section data, estimates that followed for this transport ranged from a maximum of 218 eastward [*Gordon*, 1967] to a minimum of 5 Sv westward [*Foster*, 1972]. This uncertainty was due in part to the very limited number of observations available for deriving transport (and almost complete lack of knowledge of the degree of variability in ACC transport, and hence how significant aliasing might be), and also to a lack of comprehension of how best to reference geostrophic shears to determine total transport. As noted by *Peterson* [1988a], a single section across Drake Passage (undertaken by the *Ob* in 1958) yielded ten different estimates for ACC transport, varying between 218 [*Gordon*, 1967] and just 9 Sv [*Ostapoff*, 1961].

[17] Despite the large range in transport estimates obtained during this period, *Reid and Nowlin* [1971] noted that such estimates actually became remarkably consistent when the data were handled and referenced in the same way. This is in accord with current thinking about the stability of the ACC transport, as will be seen in section 3. The uncertainty in how best to reference the geostrophic shears remained however, prompting deployment of current meters to make direct velocity measurements. A number of deep current meter moorings were deployed in Drake Passage for 4 days in 1969, giving daily mean current speeds ranging from 0.5 to 14.7 cm s^{-1}. Confusingly, this exercise actually led to an increase in the range of transport estimates, with a maximum transport of 237 Sv derived [*Reid and Nowlin*, 1971]. It later became clear that this was due to incom-

plete knowledge of the spatial and temporal variability of the ACC at Drake Passage, and the need to resolve the pertinent scales of both if direct referencing was to prove effective.

2.1. Transport and Variability From the International Southern Ocean Studies Program

[18] On the basis of the early works described above, it became clear that a dedicated program of measurements that resolved the relevant scales of variability in Drake Passage was needed, if the ACC transport and variability there were to be adequately determined. Accordingly, the ISOS program [*Nowlin et al.*, 1977] was designed and conducted, the centerpiece of which was a large monitoring array (Figure 3, top right), supplemented with hydrographic sections. (The reports of the ISOS measurements are spread over a number of papers, but are conveniently summarized by *Cunningham et al.* [2003], who also summarize the methods used in the ISOS calculations.)

[19] The specific goals of ISOS were to resolve the structure of the ACC and to obtain a yearlong time series of ACC transport. With regard to the former, analyses of ISOS and pre-ISOS data around this time led to the now well-established notion of the ACC being a banded structure, with relatively fast-flowing currents associated with frontal regions, which are themselves separated by relatively quiescent zones of water. Three narrow frontal regions were identified, and termed (north to south) the Subantarctic Front (SAF), the Polar Front (PF), and the Continental Water Boundary [*Nowlin et al.*, 1977; *Nowlin and Clifford*, 1982; *Whitworth*, 1980]. The nomenclature for the first two of these has survived, while the latter has, in general, been superseded [*Orsi et al.*, 1995].

[20] The first substantial field effort as part of ISOS was termed the First Dynamic Response and Kinematics Experiment in 1975 (FDRAKE 75), which has a good claim to being the beginning of the modern era of measurements in Drake Passage. Preliminary estimates of volume transport based on these data were in good agreement, being 110–138 [*Nowlin et al.*, 1977], 139 ± 36 [*Bryden and Pillsbury*, 1977], and 127 ± 14 Sv [*Fandry and Pillsbury*, 1979]. It was recognized that the previous poor agreement of transport estimates was due to the undersampling of reference velocities, which presented a particular problem given the greatly meandering nature of the ACC fronts, and their tendency to spawn isolated eddies [*Legeckis*, 1977; *Sciremammano*, 1979].

[21] FDRAKE 75 and the following FDRAKE 76 were precursors to the extensive ISOS deployments in 1979, and it was this latter campaign that enabled the yearlong series of transport required by ISOS to be derived (Figure 4, top). The monitoring experiment consisted of three separate hydrographic surveys, and the deployment of 17 current meter moorings deployed between the northern and southern 500 m isobaths, and bottom pressure gauges located at 500 m. The volume transport of the upper 2500 m was estimated to be 121 Sv with ~10% uncertainty, while the total transport through the whole cross-sectional area of the Passage was calculated to be between 118 and 146 Sv [*Whitworth*, 1983].
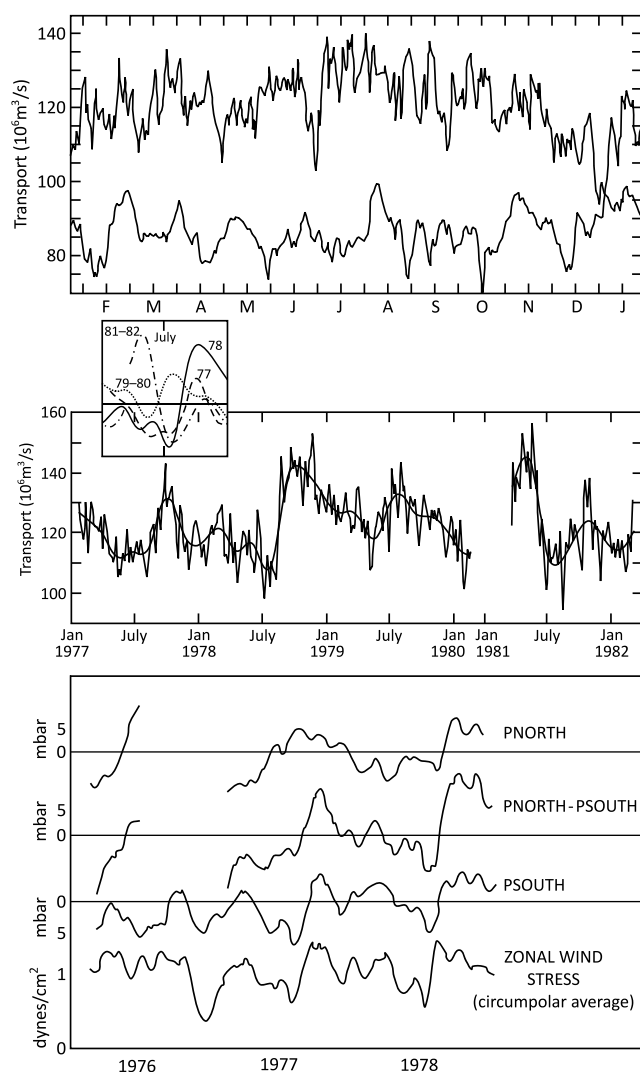
Figure 4. (top) One year transport time series through Drake Passage from ISOS (redrawn from *Whitworth* [1983]), showing the net transport (upper) and baroclinic transport of the top 2500 m (lower). (middle) Extended transport time series through Drake Passage from ISOS (redrawn from *Whitworth and Peterson* [1985]). (bottom) Low-pass filtered zonally averaged eastward wind stress and ISOS bottom pressure and cross-passage pressure difference [after *Wearn and Baker*, 1980].

The baroclinic mode was found to be responsible for 70% of the net transport, although the transport fluctuations were found to occur predominantly in the barotropic mode. This was in agreement with the earlier assertion [*Reid and Nowlin*, 1971] that the internal pressure field at Drake Passage is rather stable.

[22] The 121 Sv estimate for ACC transport was later refined to 123 Sv by *Whitworth and Peterson* [1985]. These authors also extended the ISOS transport time series using 2 additional years of bottom pressure data obtained at 500 m depth at either side of the passage (Figure 4, middle). Their calculation was based on the assumption that the transport variability was predominantly barotropic and therefore well represented by the bottom pressure data alone. (In 1979,

there was a maximum difference in transport of 24 Sv between the net transport and the transport estimated from the across-passage pressure difference, which was seen to be acceptably small.) They concluded that the variability in the transport through the passage was of the order of 10 Sv, and they noted two examples (in July 1978 and June–July 1981) of transport fluctuations approaching 50% of the mean (or approximately 50 Sv) over periods as short as 2 weeks (Figure 4, middle). The veracity of at least one of these sudden shifts in transport was later questioned (see section 3).

[23] With the intention of further extending the ISOS transport time series, *Peterson* [1988b] compared information obtained from the ISOS bottom pressure measurements with coastal sea level data obtained from tide gauges at either side of Drake Passage. Sea level at Puerto Williams in Tierra del Fuego was found to have little correspondence with the bottom pressure recorder (BPR) data on the north side of Drake Passage, apparently due to local winds for periods under 100 days and to annual changes in upper layer density. Conversely, sea level data from Faraday (now called Vernadsky) on the Antarctic Peninsula were found to be coherent with bottom pressure measurements from the south side of Drake Passage on time scales of 6–600 days. Notwithstanding this, *Peterson* [1988b] stated that "barotropic changes in transport cannot be directly estimated using these surface observations" because of a perceived phase difference between the two data sets at certain frequencies. This conclusion has since been revisited through WOCE-era studies, discussed in section 3.

2.2. Studies of Wind-Forced Transport Variability During ISOS

[24] A number of studies used the ISOS transport time series to attempt to better elucidate the dynamics of the ACC wind forcing. The 3 year ISOS transport time series was used by *Wearn and Baker* [1980], alongside wind data obtained from the Australian Bureau of Meteorology. While no studies of the accuracy of the wind data had at that time been conducted, this was nonetheless believed to be the most reliable data set available that spanned the southern hemisphere. Zonally averaged eastward wind stress between 43°S and 65°S was calculated, and compared with the ISOS bottom pressure data and transport time series (Figure 4, bottom). On the basis of the significant relationships found, a conceptual model was created whereby winds supply momentum to the ocean, which is removed by a dissipative force representing bottom friction, form drag or lateral friction. Since momentum input and dissipation are both large, the ocean system is able to respond rapidly to changes in atmospheric forcing: The expected response time of transport to a change in winds or dissipation was found to be about 7 days.

[25] Particularly noteworthy is that the significant correlation between the zonal winds and bottom pressure difference across Drake Passage determined by *Wearn and Baker* [1980] was due almost entirely to the very strong correlation with pressure at the south side of the passage. Bottom pressure at the north side bore very little resemblance to the

wind data. No convincing explanation was offered for this, though some possibilities (including seasonal density changes in the north) were suggested. This has relevance to the greater dynamic understanding of the nature of the bottom pressure variability, as discussed in section 3.

[26] A critique of *Wearn and Baker* [1980] was given by *Chelton* [1982], who made the observation that strong correlations between the bottom pressure and wind data sets could be the result of significant seasonality in both data sets, rather than evidence of a causal relationship. However, a number of more recent studies have addressed this by investigating the relationship between zonal winds and transport in the frequency domain rather than the temporal domain, with convincing results (see section 3).

[27] A number of investigations were conducted that used ISOS data to investigate other possibilities for wind forcing of transport changes. *Peterson* [1988a] derived zonally averaged wind stress curl in latitude bands at the northern and southern sides of the ACC and conducted cross-spectral analyses with the ISOS bottom pressure data. The underlying theory was that the time-varying wind stress curl in these bands would differentially force meridional movements of mass into the ACC flanks and hence alter the cross-ACC pressure gradient and thus its transport. Significant coherence was observed across a range of frequencies, and the seasonality in the bottom pressure data was seen to match reasonably well that in the corresponding wind stress curl field. Further to this, *Johnson* [1989] investigated the possibility that changes in the latitude of zero wind stress curl could be a primary driver of changes in transport through Drake Passage. Again, a reasonable level of agreement was found between the ISOS bottom pressure and transport data and the derived time series of the zero wind stress curl latitude.

[28] In retrospect, the range of significant relationships identified between winds and ISOS bottom pressure is perhaps only to be expected; each of the putative meteorological forcings examined were different measures of the same changing wind field, so (if the transport changes were to some level wind forced) some degree of correlation or coherence with a range of derived parameters is not surprising. In practice, the debate about the nature of wind forcing of the ACC transport variability was not settled on the basis of ISOS measurements, though significant further progress was made following dynamical investigations conducted alongside WOCE-era measurements (section 3).

[29] In summary, ISOS was a landmark experiment that laid much of the foundations for our current understanding of the ACC at Drake Passage. Significant results included the first detailed descriptions of the ACC zonation, the first comprehensive characterizations of its spatiotemporal variability, the first robust insights into ACC transport variability, and some early insights into the nature of wind-forced variability in the Southern Ocean. Needless to say, science progresses, and some of the ISOS findings have since been superseded, including refinements of the level of transport variability, better understanding of the dynamical nature of the transport variability, and a clearer idea of which

processes the bottom pressure measurements are actually reflecting. Many of these newer insights were made from measurements instigated during WOCE, discussed next, but it should be noted that the design of WOCE-era monitoring at Drake Passage was strongly influenced by ISOS experiences and results, highlighting the ISOS legacy.

3. SUSTAINED MONITORING IMPLEMENTED DURING WOCE

[30] The World Ocean Circulation Experiment (WOCE) was the largest international physical oceanographic program ever conducted. It coordinated the research of nearly 30 countries in making then-unprecedented in situ observations of the global ocean between 1990 and 1998. This activity in gathering in situ data was coordinated temporally with some particularly important satellite missions, including the first precise radar altimeters (ERS-1 and TOPEX/POSEIDON).

[31] The field phase of WOCE had two primary goals. The first was to develop models useful for predicting climate change and to collect the data necessary to test them. The second was to determine the representativeness of the WOCE data sets for describing the long-term behavior of the ocean, and to find methods for determining long-term changes in the ocean circulation. WOCE planning included a strategy for achieving both goals in terms of three core projects, one of which focused specifically on the Southern Ocean. Within this, targeted plans for monitoring the ACC at its Drake Passage, African and Australian "choke points" were implemented. Southern Ocean research during WOCE has since been presented in a number of special publications [*King*, 2001; *Siedler et al.*, 2001]; here we focus specifically on the sustained measurements that were initiated at Drake Passage during WOCE, and, looking back with several years' hindsight, what has been learned from them.

3.1. Bottom Pressure and Tide Gauge Measurements During WOCE

3.1.1. Variability on Subannual Periods

[32] The observational effort at Drake Passage during WOCE was predominantly led by the UK, though with other nations contributing significantly. This included the instigation of annual repeat hydrographic sections (described in detail in section 3.2; see also Figure 3, bottom left), and, following ISOS, the resumption of sustained bottom pressure measurements at the flanks of Drake Passage. These latter measurements were the responsibility of the Proudman Oceanographic Laboratory ((POL) now called the National Oceanography Centre, Liverpool), whose expertise in such measurements derived from the work of David Cartwright and colleagues in measuring tides in the deep ocean. (See *Cartwright* [1999] for an excellent review of the development of bottom pressure recording in several countries.)

[33] POL made its first set of deployments of BPR pop-up recorders across Drake Passage in November 1988, taking advantage of ship access provided by the British Antarctic Survey. These early deployments were on a line between the

Falkland Islands and the South Orkneys (Figure 3, bottom left), after which the deployments were moved close to the narrowest part of the Passage (the original WOCE "SR1" section). Since then, recorders have been deployed at each end of a line further to the east, dubbed "SR1b." Most SR1b deployments were at the WOCE standard depth of 1000 m. Additional sensors, including the long deployment (~5 years) Multiyear Return Tidal Level Equipment (MYRTLE) instrument [*Spencer and Foden*, 1996], were deployed in certain years at locations between the two ends of SR1 or SR1b.

[34] Data from the first few years of POL Drake Passage deployments were used by *Meredith et al.* [1996], who suggested that the standard deviation in transport through the Passage was between 5 and 9 Sv, compared with the 10 Sv observed in ISOS. A small part of this difference was attributable to the methods employed for dealing with end points in the data, caused when the BPRs were recovered and redeployed, though more significant was the absence of evidence for large, sudden changes in transport of the sort that were reported to have occurred twice during ISOS [*Whitworth and Peterson*, 1985]. These ISOS events were reported to have featured a change in ACC transport of up to half its mean in the space of just a couple of weeks.

[35] The absence of any similar shifts in the WOCE BPR data prompted reexamination of these events in the ISOS data, and it was noted that their temporal correspondence to changes in wind forcing was not strong, despite the pressure series (and the southside data in particular) being strongly related to winds from the data series as a whole [*Meredith et al.*, 1996]. An incontrovertible explanation for the sudden shifts reported during ISOS could not be found, and probably never will be. It was noted, however, that POL BPRs had suffered at least one event of "slippage" up to that time, whereby the gauge slid down the continental slope a little way, before settling at a deeper level. This is evident in the data as a rapid, sudden increase in pressure, unrelated to changes in the winds. (Such slippage can cause apparent transport changes of either sign, depending on whether it occurs in a northside or southside BPR.) When spotted, it is relatively easy to correct for, but if the slippage were relatively small, it would be easy to misinterpret as a genuine geophysical signal.

[36] The SR1b line was chosen to lie along an ascending track of the 35 day repeat orbit of the ERS-1 mission. Concurrently, the 10 day repeat orbit of the TOPEX/POSEIDON mission had a sufficiently high inclination to provide coverage of the Passage. Several studies were undertaken in which in situ and altimeter data were used in complementary ways. However, the results of *Woodworth et al.* [1996] and *Hughes et al.* [2003] indicated that, while altimetric measurements in Drake Passage can reveal signals of interest, questions concerning altimetric accuracy and limitations of data coverage due to winter sea ice mean that satellite measurements cannot be used as direct replacements for in situ data in estimating transport. The inadequacy of altimetric sampling, and aliasing of sea level and

transport signals, was further explored by *Gille and Hughes* [2001] and *Meredith and Hughes* [2005].

[37] Because monitoring at the three ACC chokepoints was conducted simultaneously during WOCE, a natural investigation was to study the correlation between pressure data between these locations. This was extended to include data from coastal tide gauges around Antarctica, and a high level of circumpolar coherence was found at time scales shorter than seasonal [*Aoki*, 2002; *Hughes et al.*, 2003] (Figure 5). This coherent variability was strongly correlated with the circumpolar westerly winds, as quantified by the Southern Annular Mode (SAM) [*Thompson and Wallace*, 2000]. The relevance of this circumpolarly coherent mode to the flow through Drake Passage was confirmed by comparison with transport here predicted from the 1/4° OCCAM general circulation model [*Webb*, 1998].

[38] A small number of the POL BPRs were also equipped with inverted echo sounders (IESs), with the purpose of monitoring the integrated water column properties (temperature, predominantly) as well as the bottom pressure [*Meredith et al.*, 1997]. These showed that pressure changes at the south side of Drake Passage were almost purely barotropic in nature, in that the overlying density of the water column was almost invariant over the time scales covered by the length of data. Conversely, bottom pressure at the north side of Drake Passage was more affected by water column density changes, raising questions as to how well these data relate to transport. (*Meredith et al.* [1997] argued that the standard deviation in transport derived from pairs of gauges at either side of the Passage should best be viewed as upper limits to the true transport variability.) Such findings prompted more detailed investigations into the complexity of the bottom pressure series at Drake Passage, and what processes the data were really reflecting.

3.1.2. Understanding the Dynamics of the Bottom Pressure Signals

[39] Coincident with the WOCE observational campaign in the 1990s, ocean modeling was rapidly developing, with the first large-scale eddy-permitting ocean models appearing. This made possible a more realistic examination of the interpretation of observations made in an energetic, turbulent ocean. The ISOS observations had been interpreted using a very simple flat-bottomed wind-driven channel model [*Peterson*, 1988a; *Wearn and Baker*, 1980], the essentials of which are still the basis for interpretation of observations today: Zonal wind stress produces an accelerating zonal flow, which ceases to accelerate over some characteristic decay time scale, typically about 3–10 days. However, topography must be a strong controlling factor for these transport fluctuations, and furthermore it was not clear that the large-scale processes normally considered in analytical and coarse resolution numerical models would be the dominant processes determining what is measured at a single point in the ocean. New models such as the Fine Resolution Antarctic Model [*FRAM*, 1991] and the Parallel Ocean Climate Model (POCM) [*Tokmakian and Challenor*, 1999], with Southern Ocean resolutions of about 25 km,

a)

b)

Monthly mean subsurface or bottom pressure, annual cycle removed
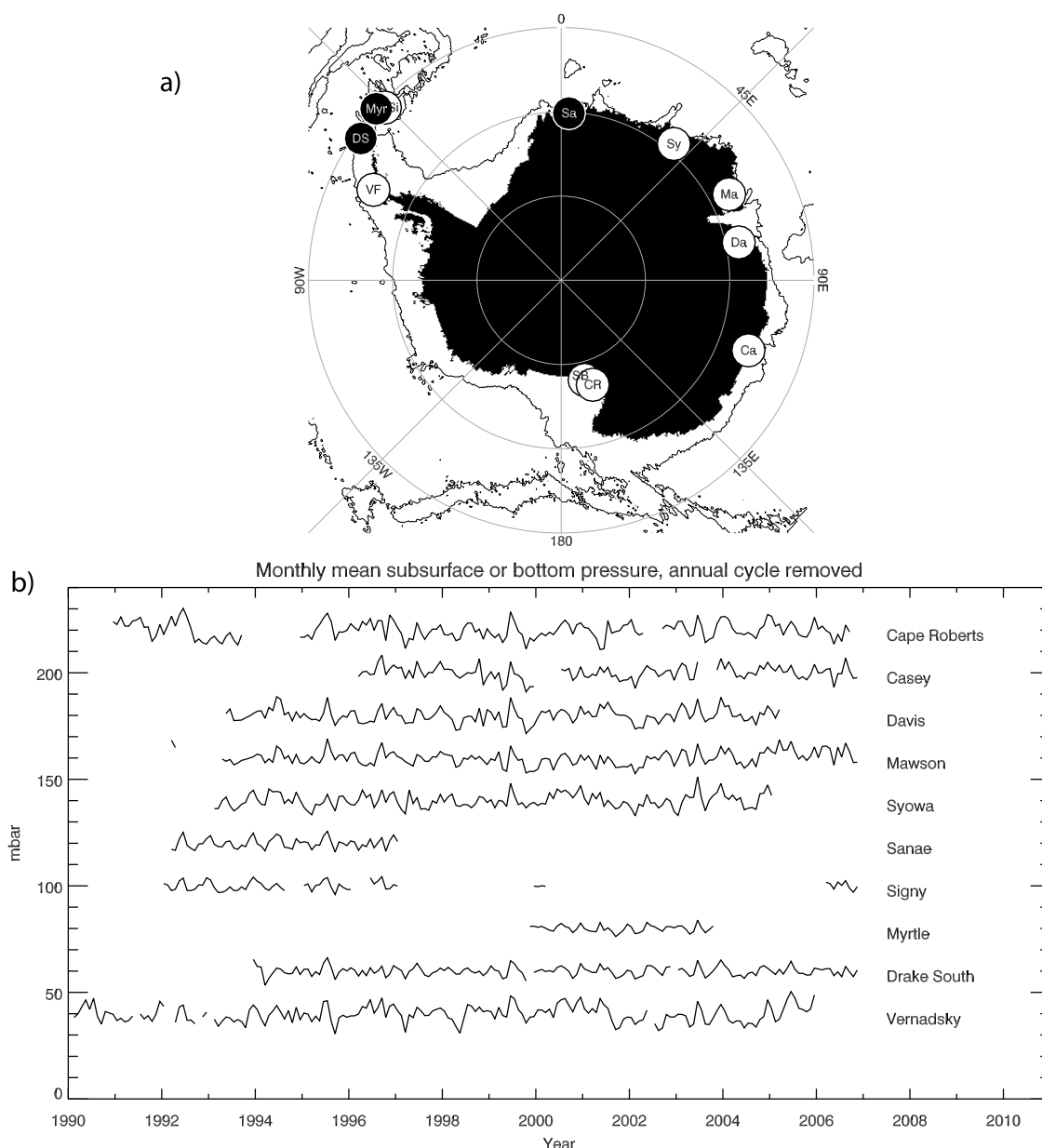
Figure 5. (a) Map showing the positions of tide gauges (white) and bottom pressure recorders (black) for which long records are available: VF, Vernadsky-Faraday; DS, Drake South (1000 m); Myr, Myrtle (2354 m); Si, Signy; Sa, Sanae; Sy, Syowa; Ma, Mawson; Da, Davis; Ca, Casey; CR, Cape Roberts; SB, Scott Base. Measurements for which a depth is not given are coastal. The 3000 m depth contour is also shown. (b) Time series [from *Hibbert et al.*, 2010] of monthly mean bottom pressures or inverse barometer corrected sea levels from the sites shown in Figure 5a. Each time series has been detrended, and an annual sinusoid has been removed by least squares fitting. The Cape Roberts time series is a composite of data from Cape Roberts and Scott Base.

could begin to reproduce the energetic eddy field of the ocean and its effect on observations.

[40] *Hughes et al.* [1999] used these models, together with WOCE BPR and tide gauge data, to investigate the relationship between Drake Passage pressure measurements and ACC transport. It became apparent that, in an eddying ocean, a meaningful definition of the northern boundary of the ACC cannot be found except in the choke points, most notably, Drake Passage. Scaling arguments also showed that, at length scales of more than a few hundred kilometers, fluctuations in

Southern Ocean currents must be predominantly barotropic on time scales shorter than about a year. This means that fluctuations in the flow will be strongly controlled by the geometry of f/H contours (f is the Coriolis parameter; H is depth), and will not follow the path of the mean ACC, which is much more weakly (though still significantly) steered by topography. With this in mind, the channel model concept had to be reinterpreted: Whereas all Drake Passage latitudes can be considered "open" in a flat-bottomed channel (i.e., these latitudes represent closed f contours), the only "open" part of
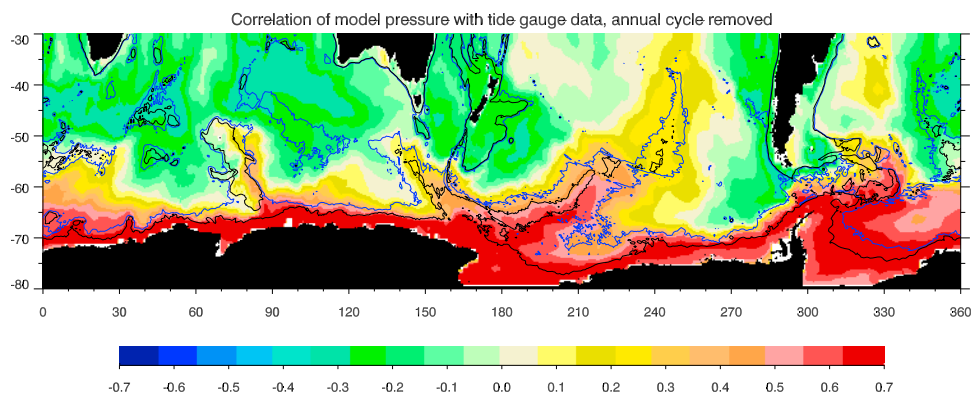
Figure 6. Geometry of the southern mode, as shown by the correlation of monthly mean values of bottom pressure in a barotropic model [*Hughes and Stepanov*, 2004] with tide gauge data. The tide gauge time series is the average of those data available (from Figure 5) at each time over the period 1992–1999. Annual cycles have been removed from each time series before correlating. Contours show the f/H contours, which correspond to depths of 3000 (black) and 4000 m (blue) at 60°S.

a Southern Ocean with topography is the narrow band of closed f/H contours that pass right around Antarctica, mostly lying along the Antarctic continental slope.

[41] The suggestion was, therefore, that fluctuations in circumpolar transport should be predominantly associated with a barotropic flow along, or near to, these closed f/H contours. Fluctuations should be driven by wind stress acting along those contours, and should be detectable (if not masked by small-scale local disturbances) in terms of bottom pressure and sea level variations on and near the Antarctic continental slope. This prediction was borne out within the models, which clearly showed such a mode [*Hughes et al.*, 1999; *Woodworth et al.*, 1996]. Comparison between models and observations of bottom pressure, sea level and wind stress were also consistent with this interpretation (Figure 6). A subtlety, which is still a subject worth investigating in more detail, is that there appears to be rather little transport associated with the "free mode" associated with the completely closed f/H contours. Most of the transport is in an "almost-free mode," which requires the current to cross f/H contours in order to pass through Drake Passage, but is clearly closely associated with the region of closed contours.

[42] The dominance of this "southern mode" of variability in Antarctic transport has been supported by subsequent observations and model investigations [*Kusahara and Ohshima*, 2009; *Vivier et al.*, 2005; *Weijer and Gille*, 2005]. The essentially barotropic nature of this mode is confirmed by comparison between barotropic and three-dimensional models, which produce very similar time series at intra-annual periods [*Hughes et al.*, 2003], and by the success of purely barotropic models in reproducing tide gauge observations [*Hibbert et al.*, 2010; *Hughes and Stepanov*, 2004; *Kusahara and Ohshima*, 2009]. At interannual time scales, however, barotropic models do not perform well, suggesting the increasing importance of baroclinic processes at lower frequencies [*Meredith et al.*, 2004].

[43] Notwithstanding the limitations of satellite altimeter data mentioned above, the part of the southern mode that extends beyond the sea ice can be seen in such data, and

matches the model predictions well [*Hughes et al.*, 2003; *Hughes and Meredith*, 2006; *Vivier et al.*, 2005]. More recently, large-scale bottom pressure variations have been measured from space by the Gravity Recovery and Climate Experiment (GRACE) satellite gravity mission, and a rather blurred version of the southern mode has also been found as the dominant Southern Ocean mode in these measurements [*Ponte and Quinn*, 2009].

[44] While the southern mode is seen to be the dominant structure associated with circumpolar transport fluctuations, it does not explain all the variability. In fact, at Drake Passage, the relationship between pressure to the south and total transport implies that the flow (if geostrophic) is occurring at larger values of H (or smaller values of f) than any that occur within Drake Passage [*Hughes et al.*, 1999]. Pressure on the northern side of the choke point must also be considered to complete the picture. However, variability on the northern side is much more complicated, and therefore harder to sample adequately. For a purely barotropic flow, the transport can be calculated from the near-bottom velocity multiplied by depth, and integrated across the channel. The baroclinic component of the flow can then be defined as the integral of the flow relative to the bottom, using thermal wind balance. Although the southern mode is highly barotropic and coherent both around Antarctica and across the Antarctic continental slope, the baroclinic contribution to transport fluctuations in FRAM was found to be significant and highly variable from place to place [e.g., *Hughes et al.*, 1999, Figure 6]. This is a result of small-scale, baroclinic processes occurring near the northern boundary.

[45] A hint as to the origin of these processes was given by *Vivier et al.* [2001] and *Vivier and Provost* [1999], who found signals on the Argentinean continental slope near 41°S that they suggested may be shelf waves originating in the Pacific and propagating through Drake Passage. This interpretation was supported by altimeter measurements [*Hughes and Meredith*, 2006], which clearly showed that signals of equatorial Pacific origin penetrate well into the Atlantic along the South American continental shelf and slope. These are not
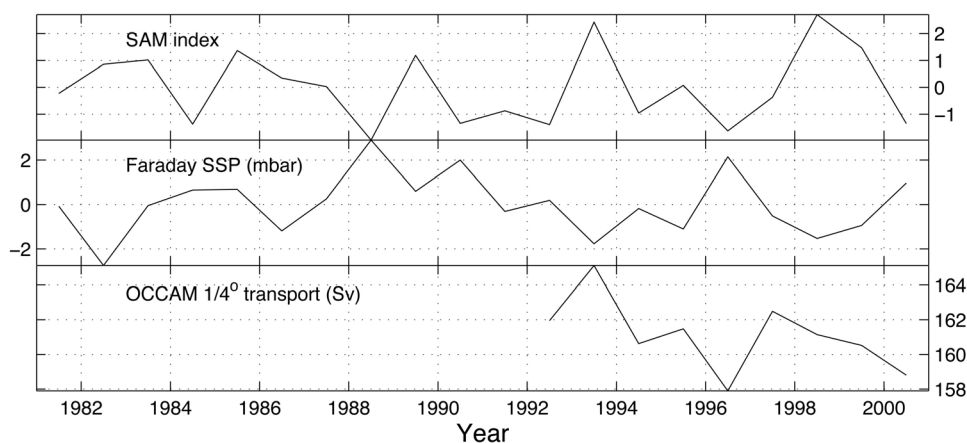
Figure 7. Annual mean time series of (top) the SAM index, (middle) atmospheric pressure corrected sea level from the Faraday tide gauge, and (bottom) transport through Drake Passage from the quarter degree OCCAM model. Note the significant anticorrelation between the upper two traces and the direct correlation between the upper and lower tracers. These indicate that interannual changes in ACC transport through Drake Passage are forced by changes in the SAM and are well monitored by sea level from the Faraday tide gauge [from *Meredith et al.*, 2004].

the only propagating signals in the northern part of Drake Passage though; as *Fetter and Matano* [2008] note, there is ample evidence for propagating eddies in this region also.

3.1.3. Interannual Variability in Transport From BPRs and Tide Gauges

[46] As noted above, the barotropic models that perform well at reproducing the subannual variability associated with the southern mode tend to perform poorly at interannual and longer periods, suggesting the increasing importance of baroclinic processes [*Meredith et al.*, 2004]. This interpretation is supported by the improved agreement with observations when using a baroclinic model with data assimilation (although not of tide gauge data), as shown by *Hibbert et al.* [2010]. The switch from barotropic to baroclinic dominance has been studied in the context of an idealized model (with realistic but somewhat smoothed topography) by *Olbers and Lettmann* [2007], who found a rather long baroclinic adjustment time scale of about 16 years, and a crossover between barotropic and baroclinic dominance at about 7–9 year periods, although this may be sensitive to the absence of eddies.

[47] Because of the presence of baroclinic variability at interannual periods, there is no a priori reason that data from a single depth in the ocean (or from a surface tide gauge) should be a reliable proxy for transport changes at these periods. Nonetheless, *Meredith et al.* [2004] investigated a long series of annual mean sea level records from the tide gauge at Faraday station (Figure 5a) on the Antarctic Peninsula in this context. (Faraday was transferred to Ukrainian control during WOCE, and renamed Vernadsky.) Data from this site represent the longest tide gauge series from Antarctica for which reliable records exist; a record extending back to the early 1980s was used for this study.

[48] The time series of sea level from Faraday showed variability that was significantly correlated with the SAM, even after correction for surface atmospheric pressure changes

(Figure 7) [*Meredith et al.*, 2004]. It was also significantly correlated with interannual changes in Drake Passage transport predicted by the full version of the 1/4° OCCAM general circulation model (though not with a purely barotropic version of the same model). This indicated that, despite the presence of baroclinic signals in the data, the Faraday tide gauge provided a reliable proxy for interannual changes in transport. This was fortuitous, and was seen to be indicative of a degree of vertical coherence in the transport changes, even though they are not purely barotropic.

[49] Of great interest is the longer-term response of the ACC to the changing SAM, since the SAM has been exhibiting a marked upward trend (stronger winds) in recent decades [*Thompson et al.*, 2000]. This has been argued to be forced at least partly by anthropogenic processes, with greenhouse gases and ozone depletion both suggested as the cause [*Marshall*, 2003; *Thompson and Solomon*, 2002], though with natural variation also contributing [e.g., *Visbeck*, 2009]. A key question remains: is the ACC strengthening as a result? Data from the Faraday tide gauge cannot answer this question, since tide gauges contain trends due to a great number of processes (isostatic rebound, global sea level rise, etc.), and isolating a trend due exclusively to a change in ACC transport is not possible. However, the BPR data from Drake Passage are useful in this context.

[50] While BPR data cannot directly inform on transport changes at periods longer than the lengths of the individual records, they do capture well the seasonal signals in the transport [*Meredith et al.*, 1996]. A significant factor in the decadal trend in the SAM is that it is not uniform across the year but is significantly seasonally modulated [*Thompson and Solomon*, 2002]. This allowed examination of the change in seasonality in Drake Passage transport in the context of the change in seasonality in the SAM over the same period; the two were seen to be strikingly similar (Figure 8). While this does not constitute direct proof that the long-term trend
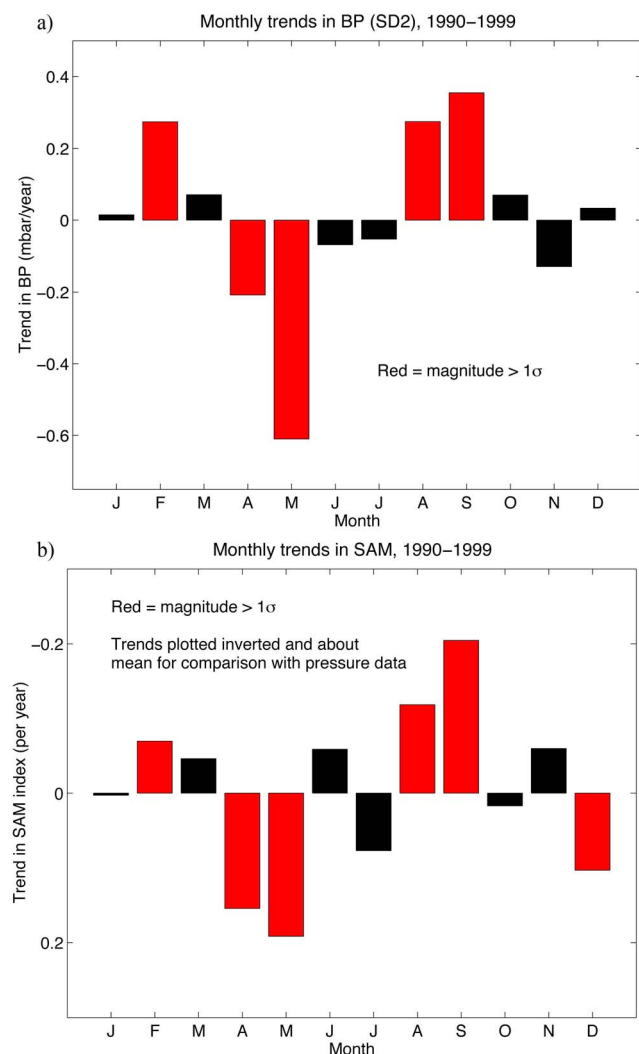
Figure 8. (a) Trends in bottom pressure from the south Drake BPR during the 1990s displayed by month. (b) Monthly trends in the SAM over the same period, here displayed inverted for comparison. Significant trends are displayed in red. The similarity between the trends indicates modulation of the seasonal cycle in transport through Drake Passage due to the changing seasonality of the SAM [from *Meredith et al.*, 2004].

in the SAM is accelerating the ACC, it is nonetheless strongly suggestive that this may be happening. Further, it was argued that, to the extent that anthropogenic processes are modulating the seasonality of the SAM, they are also influencing the flow of the ACC [*Meredith et al.*, 2004]. This proposition is discussed further in section 3.2.

[51] An interesting feature concerning the interannual changes in transport in response to the SAM is that they seem to be rather small (Figure 7), with peak-to-peak changes in transport of around 5% of the ACC mean transport, despite much larger relative changes in the overlying winds. This is consistent with more recent evidence that suggests a small-amplitude response of ACC transport with respect to winds on decadal time scales [*Böning et al.*, 2008]. These observations have helped to narrow the range of theoretical predictions regarding the dependence of ACC

transport upon the magnitude of wind stress. The upper limit of this range (over time scales for which thermodynamic equilibrium can be assumed to hold) is the linear dependence of Drake Passage transport upon wind stress [*Marshall and Radko*, 2003]; at the other end of the spectrum, *Straub* [1993] developed scaling arguments outlining parameter regimes in which transport is insensitive to the winds. The latter has become known as the "eddy saturation" limit [*Hallberg and Gnanadesikan*, 2006].

[52] Eddy saturation can be interpreted on physical grounds as the consequence of the vertical transport of momentum by eddies: In steady state, a balance exists between momentum input at the surface and momentum loss at the bottom (due to bottom form drag). When wind stress is higher, a stronger eddy field more effectively damps zonal momentum resulting in a weak dependence of transport upon wind stress. Eddy saturation theory therefore predicts that wind stress has a greater influence on eddy kinetic energy (EKE) than it does on transport; this prediction has been confirmed using satellite observations by *Meredith and Hogg* [2006] (Figure 9). Moreover, a lag of approximately 2 years between wind stress maxima and EKE is found in both observations and numerical models in the eddy saturated parameter regime, believed to be due to a slow feedback between the mean flow, eddies and topography. These findings, of relatively small variability in ACC transport on interannual and decadal time scales, have significant implications for the sampling precision and frequency that is needed when attempting to detect trends in transport (see section 3.2). These are further emphasized by theoretical arguments [*Allison et al.*, 2011] that suggest that the baroclinic ACC adjusts on centennial time scales to changes in wind stress, again consistent with *Böning et al.* [2008].

3.1.4. Relationship of Transport Changes to Low-Latitude Modes of Climate Variability

[53] As described earlier, a large-scale sea level and circumpolar transport response to variability in the SAM has been confirmed by a number of studies [*Aoki*, 2002; *Hughes et al.*, 1999, 2003; *Meredith et al.*, 2004]. However, in a more recent and perhaps surprising development, evidence has emerged that this coherent oceanic mode is also modulated by two major low-latitude atmospheric modes, namely the Madden-Julian Oscillation (MJO) [*Madden and Julian*, 1971] and the quasi-biennial oscillation (QBO) [*Angell and Korshover*, 1964].

[54] The MJO dominates intraseasonal atmospheric variability in the tropics and is characterized by the generation and eastward propagation of deep convection and precipitation anomalies on time scales of 30–100 days [*Xie and Arkin*, 1997]. A wintertime response has been identified in the extratropics in the form of planetary wave trains that extend southeastward from the tropical Pacific and Indian Oceans. Mindful of the potential influence of these upon surface wind patterns, *Matthews and Meredith* [2004] examined the SAM and Drake Passage BPR data and found an MJO component in each. Most striking was the rapidity of the transport adjustment, occurring only 3 days after the development of the extratropical atmospheric wave train.
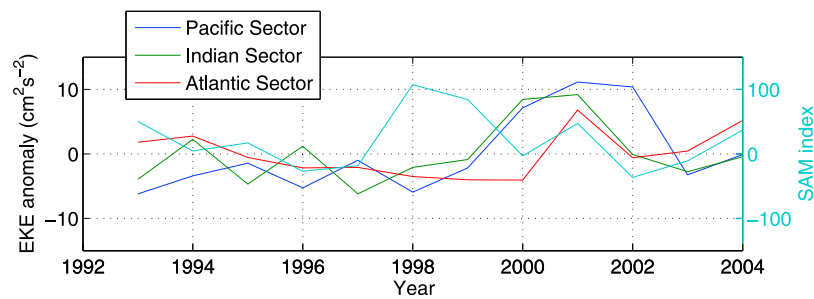
Figure 9. Annual mean changes in eddy kinetic energy (EKE) in different sectors of the Southern Ocean, plotted alongside changes in the SAM index (light blue). Note the circumpolar increase in EKE during 2000–2002, 2–3 years after an anomalous peak in SAM (redrawn from *Meredith and Hogg* [2006]).

[55] Other research has suggested that the periodic reversal in equatorial stratospheric wind direction that is described by the QBO could also influence the southern extratropical atmospheric circulation, and, when the influence of the 11 year solar cycle is taken into account, the SAM [*Roscoe and Haigh*, 2007; *Wong and Wang*, 2003]. Accordingly, *Hibbert et al.* [2010] examined whether circumpolar transport might similarly be modulated by the QBO and/or the solar cycle. They found a statistically significant QBO modulation of the Southern Ocean coherent mode and the circumpolar transport, identifying a key region of relatively weak westerly winds around 65°S via which the atmospheric signal might be communicated to the surface ocean.

[56] As with any large-scale observational program, a number of serendipitous findings were made from the Drake Passage BPR data obtained during WOCE, including detection of internal tides in the ancillary bottom temperature measurements [*Heywood et al.*, 2007], and the first detection of ventilation of intermediate and deep layers at the south side of Drake Passage by local downslope convection [*Meredith et al.*, 2003]. In addition, recent studies have demonstrated the usefulness of Drake Passage bottom pressure data for characterizing the 2004 Sumatra tsunami [*Rabinovich et al.*, 2011] and also for generating understanding of the processes that control sea level in coastal and island tide gauges so that correct attribution can be made [e.g., *Woodworth et al.*, 2005]. While interesting, these were peripheral to the core strategic aims of the WOCE monitoring program, and thus are not discussed in detail here, but the extra scientific value that such findings add to the sustained measurement program should not be underestimated.

### 3.2. Results From Hydrographic Data

3.2.1. Transports and Fluxes

[57] For WOCE, a repeat hydrographic section was initiated by the UK in the 1993–1994 season, on the SR1b line that had already been adopted for BPR measurements (Figure 3, bottom left). As with the BPR deployments, these CTD measurements were made opportunistically from RRS *James Clark Ross*, on logistics passages to or from British Antarctic Survey bases in the Antarctic. As reviewed in section 2, the definitive estimates of Drake Passage transport prior to WOCE were from ISOS: A canonical value of 134 ± 11.2 Sv was quoted by *Whitworth and Peterson* [1985], with the variation being the standard deviation of a yearlong data set, rather than the formal uncertainty of the estimate of the mean.

[58] The WOCE SR1b hydrographic section consisted of 30 full-depth CTD stations, with salinity calibrated using up to 12 bottle salinities per station analyzed on board. These sections have been continued post-WOCE, and a full description of the data and analysis is given by B. A. King and L. Jullion (manuscript in preparation, 2011). For completeness, we report here a summary of their analyses and results, including data up to the most recent cruise in November 2009.

[59] Data were collected in every southern summer season since 1993–1994, except for 1995–1996 and 1998–1999, when the CTD work could not be accommodated in the logistics schedule. Two sections were completed in 2008–2009: The first was the usual CTD-only section, the second was a full CLIVAR/GO-SHIP repeat hydrography cruise with a suite of additional chemical measurements. Wherever possible, the sections were exact repeats, with the same nominal station positions every year.

[60] Many of the cruises acquired shipboard or lowered ADCP data. While it would be possible to consider these data sets as a means of estimating the absolute water velocities (and hence a potential means of deriving total volume transport), this was decided against here primarily because the data are not available for all the early cruises, and to make partial use would compromise the comparison between years. (The referencing of transports using lowered ADCP data is discussed further in section 4). The transports reported here are thus based on the simplest possible calculation, whereby geostrophic velocities between adjacent stations are calculated relative to a presumed level of no motion at the deepest common level. No attempt was made to adjust for the contributions missed due to "bottom triangles." Volume flux was then calculated by integration of the product of the velocity and the relevant cross-sectional area. The transport calculated by this method thus represents the baroclinic structure of the ACC, and any changes in that structure, rather than being a measure of absolute ACC transport.
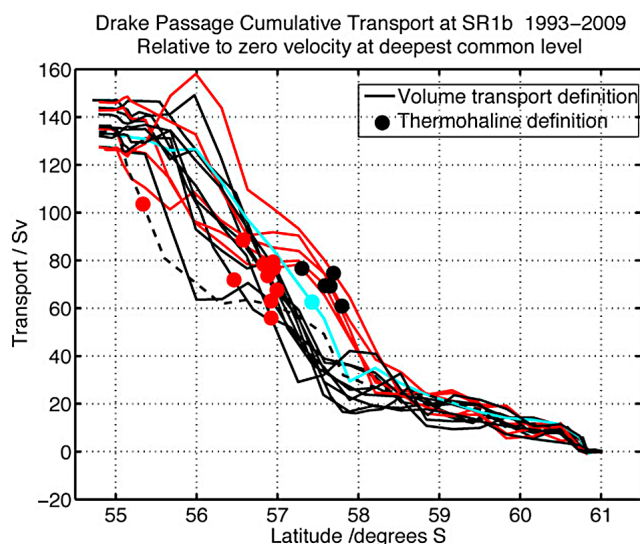
Figure 10. Cumulative transport across Drake Passage, accumulated south to north, for the 15 UK repeat hydrography cruises. The PF is bimodal in location, with the 5 "southern" years (1993–1994, 1996–1997, 2000–2001, 2003–2004, and 2006–2007) marked as red lines, an intermediate year (2005–2006) marked in cyan, and "northern" years marked in black (King and Jullion, manuscript in preparation, 2011).

[61] We have departed from this simple calculation just once: for the 2009–2010 cruise. In this year, the PF was found to be exceptionally far north, as shown by the dashed line and overlaid symbol in Figure 10. The PF-SAF system was pushed right up onto the slope near Burdwood Bank, and a reference level of zero at the deepest common level is inappropriate. Examination of the lowered ADCP data for stations north of 55.5°S suggested that near-bottom eastward velocities up to 30 cm s^{-1} were present. To allow for this, the velocity field was set to have a cross-track component of 15 cm s^{-1} at the deepest common level for stations north of 55.5°S for this section alone.

[62] Temperature and salinity are averaged from adjacent stations onto the derived velocity field. Temperature flux is obtained by summing the product of each volume flux element with the element's temperature in degrees Celsius (on the International Temperature Scale, 1990); this quantity is dominated by the volume flux, and it would be meaningless to interpret it as a heat flux. Instead, this temperature flux is divided by the volume flux to give a transport-weighted

mean temperature. This is referred to as simply the "mean temperature." Changes in this mean temperature enable us to estimate the change in exceptional heat flux through Drake Passage for some nominal value of the total volume flux, without requiring a bounded region with a balanced mass budget. Likewise, salt flux is obtained from the product of volume flux elements with Practical Salinity, but then reduced to a transport-weighted mean salinity.

[63] Figure 10 shows the volume flux for each cruise, accumulated from zero at the southern end of the section. The PF generally occupies the region between 58°S and 56.5°S, shown by the sharp increase in transport here. Its location is distinctly bimodal, with the 5 "southern" years (red lines) being 1993–1994, 1996–1997, 2000–2001, 2003–2004 and 2006–2007. The intermediate year (cyan line) is 2005–2006. In the southern PF years, there is a distinct transition zone between the PF and the SAF to the north. In the northern PF years (black lines), the accumulating transport is less likely to show an obvious inflexion between the fronts. The positions of the PF as defined using the thermohaline criterion (2°C isotherm crossing 200 m) of *Orsi et al.* [1995] for each cruise are also shown (black dots for the southern PF positions and red dots for the northern PF position). The dashed black line marks the most northerly position of the PF and corresponds to the exceptional year 2009–2010. Analysis of satellite altimeter and sea surface temperature data for the time of that cruise (not shown) reveals the presence of a large meander of the PF, which extended up to the continental slope of South America at that time.

[64] The mean volume transport from the 16 sections is 136.7 Sv, with a standard deviation of 6.9 Sv. Table 1 lists the range, mean and standard deviation of the volume flux and other quantities of interest. Figure 11 shows time series of the volume, mean temperature, and mean salinity from the 16 sections, both with (solid lines) and without (dashed) a seasonal adjustment (described in this section). The most striking features of the unadjusted time series are the high mean temperature during the 1999–2000 cruise and the second 2008–2009 cruise. This is expected, since these cruises were undertaken later in the season (February) than the others. The difference in mean temperature, 0.4°C, is equivalent to 0.2 PW when multiplied by a nominal volume flux of 137 Sv. It is therefore crucial that any attempt to close a heat budget of the Southern Ocean that involves Drake Passage sections must consider the month in which data were gathered.

TABLE 1. Minimum, Mean, Maximum, and Standard Deviation of Transports at Drake Passage for the UK Repeat Hydrography Cruises[a]

	No Seasonal Adjustment				With Seasonal Adjustment			
	Minimum	Mean	Maximum	Standard Deviation	Minimum	Mean	Maximum	Standard Deviation
Volume (Sv)	126.3	136.7	147.1	6.9	126.3	136.7	147.1	6.9
Potential temperature (°C)	2.05	2.21	2.55	0.15	1.94	2.15	2.24	0.07
Practical salinity	34.430	34.444	34.464	0.009	34.434	34.446	34.468	0.008

[a]Data are shown with and without seasonal adjustment to 1 December of each season. There is no seasonal adjustment for the volume transport, so the numbers are unchanged. The potential temperature and practical salinity are transport-weighted mean properties.
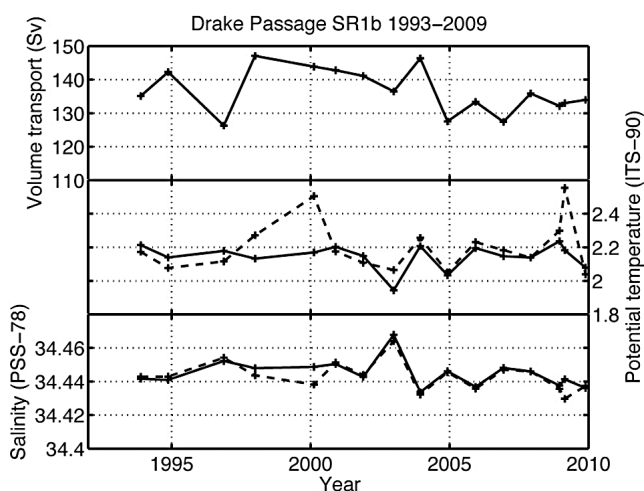
Figure 11. Time series of transports at Drake Passage for the UK repeat hydrography cruises. (top) Volume transport, (middle) transport-weighted mean temperature, (bottom) transport-weighted mean salinity. Dashed lines denote values calculated relative to the time of the cruises, and solid lines denote values following seasonal adjustment to be made relative to 1 December (from King and Jullion, manuscript in preparation, 2011).

[65] Figure 12 shows the volume flux, mean temperature and mean salinity for each section, as a function of year day. Since each set of measurements occupies up to 6 days of elapsed time, the central day of each data gathering period is used. Most of the data were gathered before, or just after, the year-end. The two February cruises provide the high values to the right of Figure 12 (middle), but even apart from these two late season cruises there is a well-resolved trend through the southern spring, shown by the solid line. The full seasonal cycle is not resolved, but the trend during spring and summer can be determined. There is no obvious seasonal variation in the total volume flux (Figure 12, top) and a weak freshening trend in the mean salinity (Figure 12, bottom). The 2002–2003 data, centered on day 362, is an outlier from the underlying seasonal trend in both mean temperature and salinity, for reasons that have not been identified.

[66] In order to look for decadal trends in transport and fluxes, a seasonal adjustment has been made to the total fluxes, using the slopes of the best fit lines in Figure 12. The slopes are 0.44°C $(100 \, \text{d})^{-1}$ for temperature and $-0.015 \, (100 \, \text{d})^{-1}$ for salinity. Total fluxes for each cruise have been adjusted to equivalent values at 1 December (day 335). The seasonally adjusted time series are the solid lines in Figure 11 (middle and bottom). As noted earlier, the 2002–2003 cruise appears as an outlier in the adjusted time series, and no explanation has yet been found. Satellite-derived sea surface temperature shows nothing unusual at the time of this cruise. The 2004–2005 cruise is also slightly cooler than other years. Apart from these, the mean temperature and salinity are remarkably stable. There is no discernable trend in any of the transports.

[67] We consider briefly the errors or uncertainty in the calculations presented in Figures 11 and 12. The contribu-

tion from measurement error is negligible. Suppose that the CTD measurements of temperature, salinity, and pressure have random errors of 0.002°C, 0.002, and 2 dbar, respectively, offset on each station. When these errors are combined the standard deviations of the changes to the mean temperature transport, mean salinity transport, and volume transport are 0.004°C, less than 0.001, and less than 0.1 Sv, respectively, an order of magnitude below the interannual variability. The error bar in each calculation in Figure 11 is thus too small to plot. In effect we have 16 precise measurements of a variable quantity, and rather than being one of errors, the issue is one of representativeness. Our 16 sections have characterized the size of the variability, but not the time scales on which it occurs.

[68] Given the apparent lack of trends, it is pertinent to ask the minimum size of change that could be detected from such annual measurements. First, we suppose that the full variance of the transport, for example, can be represented by the variance of a decade of annual measurements. This supposes that while individual realizations of the section may have aliased the higher-frequency variability, a sufficient range of higher-frequency variability has been sampled by the individual cruises: ten such measurements in our assumption. Then a two-tailed student t-test suggests that the smallest change that could be detected between two decadal means is roughly equal to the sample standard deviation in each decadal mean. We therefore conclude that the magnitude of any change in the transport or mean properties of the ACC at Drake Passage over the period of the UK repeat CTD cruises is no greater than the standard deviations in the right-hand column of Table 1. This places a useful constraint on how small the response of the ACC
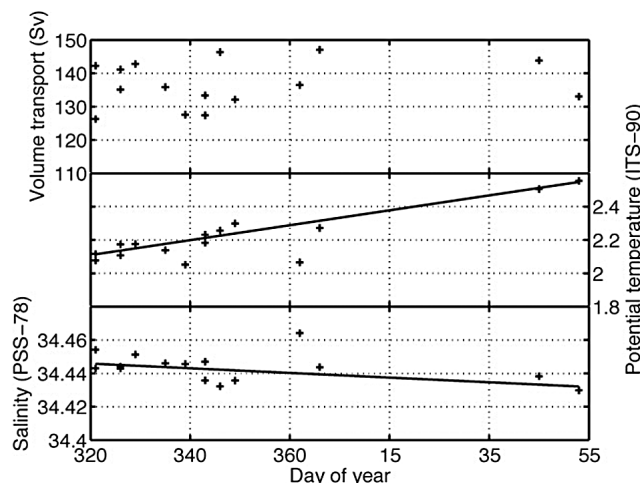
Figure 12. Seasonal variation of transports at Drake Passage for UK repeat hydrography cruises. (top) Volume transport, (middle) transport-weighted mean temperature, (bottom) transport-weighted mean salinity. The top illustration has no significant slope. The middle and bottom images show the least squares best fit used for subsequent adjustment of the data (from King and Jullion, manuscript in preparation, 2011).
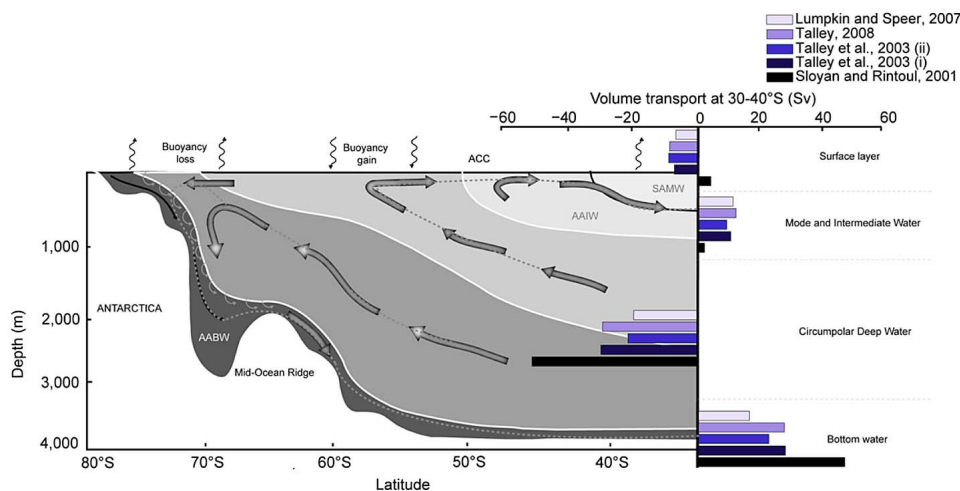
Figure 13. Schematic two-cell meridional overturning circulation in the Southern Ocean (adapted from *Speer et al.* [2000]). Five observationally based estimates of the volume transports in different water mass classes at 30°S–40°S are superimposed.

transport is to changing winds, and what impact this might have on associated property fluxes.

[69] Interestingly, the WOCE SR1b CTD data show no evidence for a southward shift of the PF (neither using the transport definition or a thermohaline definition of the PF), despite it having been argued elsewhere that the ACC could be migrating southward, associated with the climatic poleward movement of the circumpolar winds [e.g., *Gille*, 2008; *Sprintall*, 2008]. Given the constrained nature of the PF on SR1b (Figure 10), it may be that this section is unusual in this regard compared with the ACC more generally around its circumpolar path. This is discussed further in section 4.

3.2.2. The Southern Ocean Meridional Overturning Circulation

[70] As seen already (Figure 2), the horizontal circulation of the ACC is associated with a complex Southern Ocean meridional circulation that is related to the formation, modification and ventilation of the world ocean water masses. Within this overturning circulation, CDW upwells close to the surface south of the ACC, whereupon it can be pushed north under the direct influence of the winds and reenter the ocean interior as AAIW and SAMW; alternatively, it can be transformed into dense waters that become AABW close to the Antarctic continent (Figure 13).

[71] The two-cell structure of the meridional overturning circulation in the Southern Ocean was first revealed by the early descriptions of the hydrographic structure [e.g., *Deacon*, 1937]. However, because of the absence of zonal barriers and the importance of the eddy-induced flow in the overturning circulation, assessing and monitoring its intensity has been challenging. In contrast to the measurement of ACC transport, determination of the strength of the overturning circulation can only be achieved by indirect methods such as inverse models. In this respect, the repeated hydrographic sections of the WOCE era have proved very useful: In combination with the other Southern Ocean sections, they have allowed estimates of the strength of the Southern Ocean overturning circulation for the first time.

[72] To enable this, two main methods have been applied to WOCE observations: methods using geostrophic velocity data derived from hydrography with empirically chosen reference levels [e.g., *Talley et al.*, 2003; *Talley*, 2008] and box inverse methods [e.g., *Lumpkin and Speer*, 2007; *Sloyan and Rintoul*, 2001]. Significant uncertainties remain on the estimate of the strength of the overturning circulation, indeed both methods are highly sensitive to empirical choices. For instance, inverse methods depend critically on the choice of the weight matrices, which are, in practice, not possible to derive from observations. In addition, inverse solutions depend on mixing schemes used, treatment of the interactions between the ocean interior circulation and the ocean surface layer, and other critical physical mechanisms that are still not accurately understood. In turn, methods based on geostrophic velocities depend on subjective choices, for instance when adjusting observed geostrophic shear to match the observed property distribution. Notwithstanding this, the comparison of several studies that cover a range of such subjective choices can provide important information on the intensity of the Southern Ocean overturning circulation.

[73] The overturning circulation in the Southern Ocean is estimated to involve a southward transport of CDW over the circumpolar belt of between 20 Sv [*Lumpkin and Speer*, 2007] and 52 Sv [*Sloyan and Rintoul*, 2001] (Figure 13). Although both estimates arise from inverse analysis of WOCE hydrographic sections, *Lumpkin and Speer* [2007] considered twice as many layers in their inverse model as did *Sloyan and Rintoul* [2001], and the two inverse methods also use different air-sea forcing. However, *Lumpkin and Speer* [2007] suggested that the calculation of *Sloyan and Rintoul* [2001] might be biased high by the different treatment of the interaction of Ekman transport and water mass formation, rather than because of the difference in air-sea forcing. The estimates from *Talley et al.* [2003] and *Talley* [2008] from geostrophic velocity data give numbers slightly above the estimate of *Lumpkin and Speer* [2007],

with 22–30 Sv of southward transport of CDW over the circumpolar belt. Similar discrepancies exist in the transport of other water masses. These are due to a number of reasons, including the number of density layers considered, model treatment of mixing and surface layers, velocity reference levels, the error matrix, and the surface forcing. But overall, these observationally based estimates provide a generally consistent picture of the Southern Ocean overturning circulation.

[74] Additional studies have estimated the intensity of the Southern Ocean overturning, acknowledging that the transport across the ACC results from a balance between northward wind-driven flow at surface and eddy-induced flow at depth. The eddy-induced transport can be parameterized using diffusion coefficients and the climatological isopycnal structure of the ocean interior [e.g., *Gent and McWilliams*, 1990]. From the climatological isopycnal structure of the Southern Ocean, *Zika et al.* [2009] produced a quantified relationship between the magnitude of the overturning circulation and the mixing intensity in the Southern Ocean, suggesting that a mean isopycnal mixing coefficient of the order of 300 $m^2\ s^{-1}$ and a mean diapycnal mixing coefficient of the order of $10^{-4}\ m^2\ s^{-1}$ would be needed to maintain an overturning strength of the magnitude estimated by inverse methods. The overturning circulation transports are also tightly linked to water mass transformations, which can be estimated in the near-surface ocean from air-sea buoyancy fluxes [e.g., *Speer et al.*, 2000]. In the near-surface ocean, both thermodynamics and the eddy-induced parameterization method have suggested upwelling of 10–20 Sv south of the ACC, a northward meridional export, and a reinjection of 10–20 Sv within or north of the ACC [e.g., *Karsten and Marshall*, 2002; *Marshall et al.*, 2006; *Speer et al.*, 2000]. *Sallée et al.* [2010] pinpointed the regional distribution of this process, with very large subduction fluxes in SAMW and AAIW layers at Drake Passage.

### 3.2.3. Changes in Upper and Lower Limbs of the Southern Ocean Overturning

[75] In addition to contributing to information on the mean strength of overturning in the Southern Ocean, the repeat hydrography program at Drake Passage instigated during WOCE has proved especially useful for monitoring the evolution of several globally significant water masses relevant to this overturning. This is true for both the upper ocean SAMW and AAIW that ventilate the pycnocline of the Southern Hemisphere oceans [*Hanawa and Talley*, 2001] (section 3.2.2), and for the AABW that forms in the nearby Weddell Sea and that invades large areas of the global ocean abyss [*Orsi et al.*, 1999]. In the following, we review the character and driving mechanisms of the variability of these water masses, as revealed by several decades of hydrographic measurements in Drake Passage, the majority of which were collected from the WOCE SR1b line (Figure 3, bottom left).

[76] The SAMW that flows through Drake Passage is formed by winter overturning on the equatorward flank of the ACC, in a region of deep winter mixed layers in

the southeast Pacific and in the passage itself [*Naveira Garabato et al.*, 2009]. SAMW (defined here by the 26.80–27.23 kg m^{-3} neutral density range to the north of the SAF) exhibited substantial variability between 1969 and 2005 (Figure 14), with potential temperature (θ), salinity (S), and pressure changes of 0.1°C–0.4°C, 0.01–0.04, and 30–200 dbar, respectively. Positive θ and S anomalies generally covary with layer mean shoaling, thinning, and lightening (as expected from a convective formation process), and vice versa. These changes are mainly driven by variations in wintertime air-sea turbulent heat fluxes and net evaporation modulated by the El Niño–Southern Oscillation (ENSO) phenomenon and, to a lesser extent, the SAM [*Naveira Garabato et al.*, 2009]. A prominent exception to the usual buoyancy-driven overturning of SAMW formation took place in 1998, when strong wind forcing associated with constructive interference between ENSO and the SAM triggered a transitory shift to a friction-dominated mode of ventilation.

[77] The time series of SAMW properties in Figure 14 also reveals significant interdecadal changes. SAMW is seen to have warmed (by ~0.3°C) and salinified (by ~0.04) during the 1970s, with little change in density, whereas it experienced the reverse trends between 1990 and 2005, resulting in a marked lightening of ~0.06 kg m^{-3}. The coldest, freshest, and lightest SAMW is observed at the end of the time series. Available evidence (discussed by *Naveira Garabato et al.* [2009]) suggests that the reversing changes in SAMW characteristics were chiefly forced by a ~30 year oscillation in regional air-sea turbulent heat fluxes and precipitation associated with the Interdecadal Pacific Oscillation (IPO). A SAM-driven intensification of the Ekman supply of cold, fresh surface waters from the south also contributed significantly. The IPO is an interdecadal fluctuation in SST and atmospheric circulation centered over the Pacific Ocean that may result from the projection of stochastic ENSO variability onto interdecadal time scales. Its association with the interdecadal oscillation in SAMW properties is apparent from the qualitative resemblance between the property time series and the evolution of the IPO index in Figure 14.

[78] The AAIW in Drake Passage is ventilated by the northward subduction at the PF of the winter water originating in the winter mixed layer of the Bellingshausen Sea. AAIW (defined here by the 27.23–27.50 kg m^{-3} neutral density range to the north of the PF) displayed interannual variations comparable in amplitude to those of SAMW during 1969–2005 (Figure 14), but positive (negative) θ and S anomalies now covary with layer mean deepening, thinning, and lightening (shoaling, thickening, and densification). These changes stem from variations in winter water properties resulting from fluctuations in wintertime air-sea turbulent heat fluxes and spring sea ice melting, both of which depend strongly on the intensity of (partially ENSO- and SAM-forced) meridional winds to the west of the Antarctic Peninsula. Coupled with the transitory shift in the mode of SAMW ventilation, a 1–2 year shutdown of AAIW
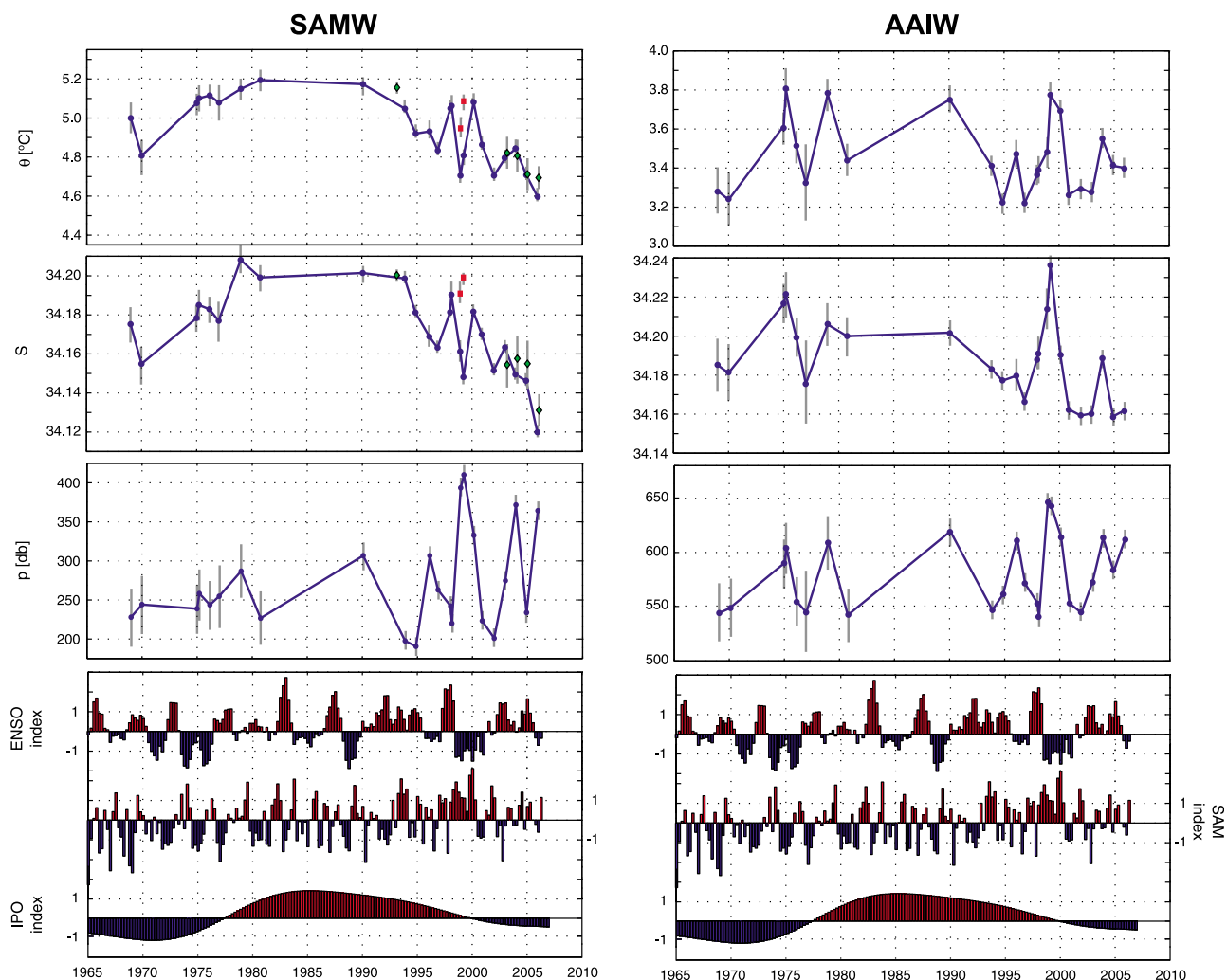
Figure 14. The first three panels show time series of potential temperature, salinity, and pressure in the Subantarctic Mode Water and Antarctic Intermediate Water layers in Drake Passage. (left) All variables show layer mean values except pressure for SAMW, which is the average value at the lower boundary of this water mass. In 1998–1999 for SAMW potential temperature and salinity, the red symbols indicate the exceptional presence of a second SAMW mode (see *Naveira Garabato et al.* [2009] for details). Error bars amalgamate systematic, standard, and sampling errors as estimated by *Naveira Garabato et al.* [2009]. The fourth panels show times series of indices of three major modes of Southern Hemisphere climate variability: ENSO, SAM, and IPO.

formation was initiated in 1998, driven by the extraordinary wind forcing of that winter. This resulted in a rapid warming and salinification of AAIW at the time (Figure 14).

[79] The interdecadal evolution of AAIW is characterized by a significant freshening of ~0.05 between the 1970s and the turn of the century, with little detectable change in θ. This freshening has been shown to stem from a freshening of the winter water in the Bellingshausen Sea [*Naveira Garabato et al.*, 2009]. Such change was brought about by increased precipitation and a retreat of the winter sea ice edge, forced by an interdecadal trend in meridional wind stress (likely associated with a concurrent positive tendency in the SAM) and regional positive feedbacks in the air-sea-ice-coupled climate system. Thus, the AAIW freshening is a deep ocean manifestation of the extreme climate change that

has occurred along the West Antarctic Peninsula in recent decades [*Meredith and King*, 2005; *Vaughan et al.*, 2003].

[80] The observed variability in the properties of SAMW and AAIW raises the question of whether the rate of subduction of those water masses (and, ultimately, the rate of meridional overturning) changes considerably in response to climatic forcing. While we have no way of directly measuring the overturning stream function from the available observations, several aspects of the measured property changes are suggestive of significant perturbations in the overturning. Consider, for example, the observed changes in the pressure of SAMW and AAIW (Figure 14), which are associated with substantial variations in the potential vorticity of those layers [*Naveira Garabato et al.*, 2009]. If we portray the Southern Ocean overturning circulation as the
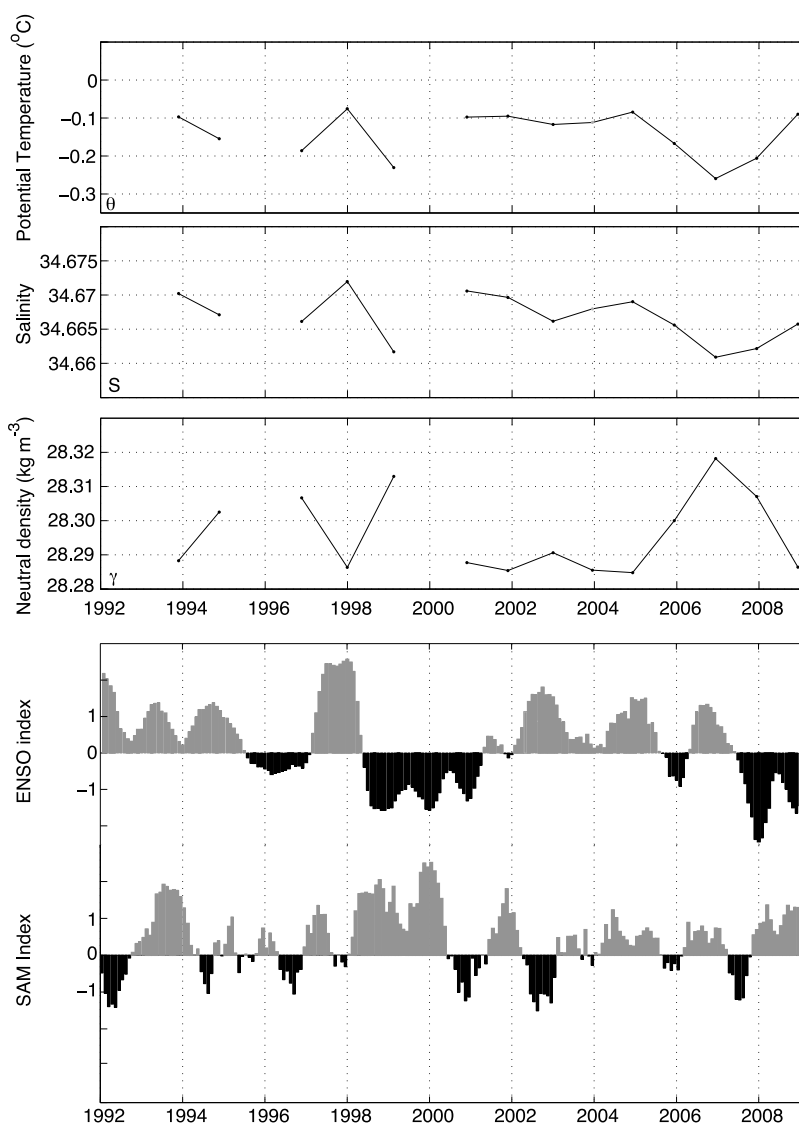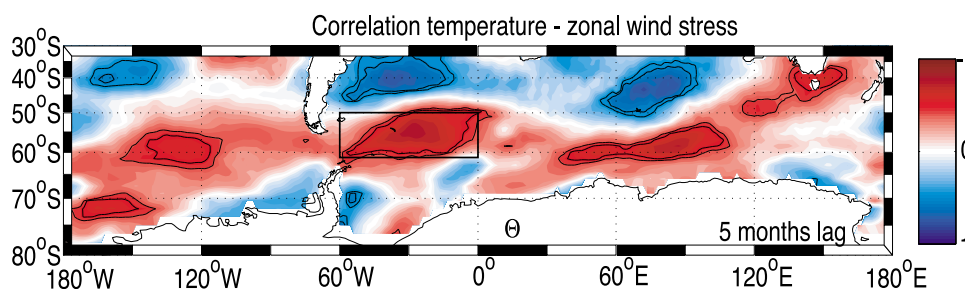
Figure 15. Time series of potential temperature, salinity, and neutral density of Antarctic Bottom Water on the WOCE SR1b section (Figure 3). Also shown are 1 year low-pass filtered ENSO and SAM indices over the same period [from *Jullion et al.*, 2010].

residual arising from the incomplete cancellation between a wind-driven Eulerian mean cell and a generally opposing eddy-induced cell [e.g., *Marshall and Radko*, 2003, 2006], we may readily conclude that the observed changes in potential vorticity are conducive to variations in eddy-induced overturning that are not necessarily countered by changes in the Eulerian mean cell (see, e.g., discussion by *Naveira Garabato et al.* [2009]). The clearest illustration of a perturbation to the overturning circulation associated with wind-forced changes in the Eulerian mean and eddy-induced flows in the Drake Passage region may be found in the 2 year period following the winter of 1998–1999. During that winter, anomalously strong upfront winds led to a striking arrest in the formation of AAIW (which ceased to be ventilated for 1–2 years, as evidenced by its anomalously warm and salty character between 1998 and 2000) and a transitory shift in the formation mechanism of SAMW (which was ventilated by a strong Ekman transport of

Antarctic surface waters from the south, as manifested in its anomalously cold and fresh character in the same period). The dynamics underpinning these changes in mode and intermediate water subduction are discussed in more detail by *Naveira Garabato et al.* [2009].

[81] The AABW found in Drake Passage is a recently ventilated variety of the water mass that leaves the Weddell Sea through clefts in the South Scotia Ridge and flows westward in a deep boundary current at the southern edge of the Scotia Sea [*Gordon et al.*, 2001; *Naveira Garabato et al.*, 2002b]. Significant variation in AABW properties and transports within the Weddell Sea has been observed, on time scales from seasonal to interannual and beyond [*Fahrbach et al.*, 2004; *Gordon et al.*, 2010; *Robertson et al.*, 2002], though the absence of a clearly defined decadal trend in AABW temperatures in the Weddell Sea seemingly conflicts with observations of significant AABW warming along the length of the Atlantic [*Johnson and Doney*, 2006; *Johnson*

Figure 16. Spatial correlation at 5 months lag between zonal wind anomalies and the potential temperature of AABW in Drake Passage (Figure 15). The black lines are the 90% and 95% significance limits. The marked zonality in the correlation field is strongly indicative of the SAM [from *Jullion et al.*, 2010].

et al., 2008; *Meredith et al.*, 2008]. Consequently, much attention has focused on understanding the processes that control the properties and flux of AABW as it exits the Weddell Sea, and Drake Passage hydrographic data have proved valuable in this context.

[82] A time series of Drake Passage AABW properties between 1993 and 2008 (Figure 15) shows significant variability, although the characteristic time scale of the measured changes is believed to be shorter than 1 year, and thus some level of aliasing must occur [*Jullion et al.*, 2010]. Notwithstanding this, the time series in Figure 15 is useful in elucidating the controls of the properties of the AABW exported from the Weddell Sea. This is demonstrated by Figure 16, which displays the correlation between the θ of AABW and the zonal wind stress over the Southern Ocean. High positive correlations occur over the northern limb of the Weddell gyre with a lag of ~5 months, suggesting that instances of stronger (weaker) wind forcing of the gyre lead to warmer (colder) AABW in Drake Passage a few months later. Examination of mooring records in the region further shows that fluctuations in wind forcing and AABW temperature occur in synchrony with variations in AABW outflow speed, with an association of anomalously strong winds and positive anomalies in AABW flow [*Meredith et al.*, 2011]. These findings are consistent with (and expand upon) the "Weddell gyre intensity" hypothesis [*Meredith et al.*, 2008], in which baroclinic adjustment of the gyre to changes in wind stress curl results in variations in the density horizon (and therefore θ and S) of the AABW overflowing the South Scotia Ridge, though they emphasize more the significance of local winds and processes within the vicinity of the South Scotia Ridge. Wind stress fluctuations along this ridge and over the broader Weddell gyre have been shown to respond substantially to changes in the SAM [*Jullion et al.*, 2010], suggesting that this coupled mode of climate variability may exert a significant influence on the properties and flux of the AABW escaping the Weddell Sea.

[83] Overall, the time series of hydrographic measurements in Drake Passage lends an important new perspective to the problem of modern global ocean climate change. On one hand, it suggests that the interdecadal freshening of SAMW and AAIW observed widely across the subtropical oceans since the 1960s [*Bindoff et al.*, 2007] may have distinctly different origins, and that the concurrent AABW warming measured across much of the Atlantic Ocean [*Johnson and Doney*, 2006; *Meredith et al.*, 2008] may have been caused by wind-driven changes in AABW export rather than modified source water properties. On the other hand, it reveals that the major modes of atmospheric variability play a key role in driving ocean climate evolution and that this forcing occurs on surprisingly short time scales (of several months, even at abyssal depths). It was only via the sustained, systematic observation of the full depth ocean that these findings were obtainable.

4. OBSERVATIONAL PROGRAMS IMPLEMENTED SINCE WOCE

[84] A legacy of WOCE is the global oceanographic data set that was collected under its auspices. WOCE raised awareness of the importance of implementing a sustained global ocean observing system (GOOS) in order to describe and understand the physical processes responsible for climate variability and to extend the range and accuracy of prediction on time scales from seasonal to decadal. A number of its programs such as repeat hydrography have continued under its immediate successor, CLIVAR (Climate Variability and Prediction). Under the umbrella of GOOS, a scientific rationale and strategy for a Southern Ocean Observing System (SOOS) (http://www.scar.org/soos/) has been proposed with recommendation for continued choke point monitoring [*Rintoul et al.*, 2010]. The 2007–2009 International Polar Year (IPY) provided a timely stimulus to the SOOS planning. Although IPY was the fourth polar year of its kind (following those in 1882–1883, 1932–1933, and 1957–1958) it was the first during which the Southern Ocean was measured in a truly comprehensive way, and it carried out some of the central observational elements proposed for the SOOS.

[85] In this section, we focus on new sustained observational programs begun in Drake Passage since the end of WOCE. These include the U.S. Drake Passage repeat expendable bathythermograph (XBT) and acoustic Doppler current profiler (ADCP) lines, the U.S. IPY cDrake array of Current and Pressure Recording Inverted Echo Sounders (CPIES), the French DRAKE program and mooring line, and the UK-U.S. DIMES program.

4.1. Drake Passage XBT-ADCP Repeat Line

[86] Year-round monitoring of upper ocean temperature variability in Drake Passage was begun in 1996 through repeat expendable bathythermograph (XBT) surveys from the United States' Antarctic supply vessel. The XBTs are dropped at intervals of 5–15 km spacing (closest spacing across the Subantarctic and Polar Fronts) between the 200 m isobaths at either side of Drake Passage on approximately 6 crossings per year [*Sprintall*, 2003]. The three most frequently repeated tracks are shown in Figure 3 (bottom right). The XBT probes consistently return water temperatures down to 850 m, with 1 m depth bins. Sampling has expanded in recent years to include expendable CTD (XCTD) probes; twelve XCTDs are deployed at intervals of 25–50 km and measure temperature and salinity to around 1000 m. XBT temperature profiles are combined with historical hydrography and XCTDs to calculate salinity profiles.

[87] Continuous upper ocean current profiling from a hull-mounted 150 kHz shipboard acoustic Doppler current profiler (ADCP) was added in September 1999; a second 38 kHz ADCP was added in late 2004. The 150 kHz ADCP provides velocity measurements at 8 m vertical resolution over a 300 m depth range. The 38 kHz ADCP provides velocity measurements at 24 m vertical resolution over a 1000 m depth range. Measurements of the atmospheric partial pressure of CO_2 (pCO_2) and dissolved CO_2 in the surface waters were added in 2003. The underway ADCP and pCO_2 observations are made on all crossings (about 20 yr^{-1}); the dissolved CO_2 surface sampling is limited to the 6 XBT transects.

4.1.1. Defining ACC Streamlines in Drake Passage

[88] While the ISOS picture of a banded frontal structure has proved to be a robust description of the mean ACC, higher-resolution measurements from ships and satellites [e.g., *Hughes and Ash*, 2001; *Sokolov and Rintoul*, 2007] have shown that the frontal structure is more complex than earlier sampling suggested. At high temporal and spatial resolution, the principal ACC fronts comprise multiple filaments that subsequently merge and diverge along the circumpolar path of the current. The multiple filaments exhibit substantial persistence in space and time, with as many as eight or nine identified in the wide chokepoint south of Tasmania [*Sokolov and Rintoul*, 2007]. Multiple filaments of the SAF, PF and Southern ACC Front (SACCF) upstream of Drake Passage converge into three main frontal jets as they enter its narrowest horizontal constriction. High-resolution sampling identifies the mean positions of the SAF and PF about 50 km north of their climatological positions [*Lenn et al.*, 2007; *Orsi et al.*, 1995]. The apparent northward displacement of the means is likely due to uncertainty in determining front locations from the coarser sampling (~50 km spacing) characteristic of the earlier period. While the Drake Passage mean ACC is dominated by three frontal jets, consistent with *Nowlin et al.* [1977], the variability is dominated by mesoscale eddies and meanders of the fronts, with smaller contributions from inertial currents and the baroclinic tide. Horizontal wave number spectra of ocean currents are consistent with aspects of geostrophic turbulence [*Lenn et al.*, 2007]. Along the repeat XBT-ADCP line, EKE is concentrated in northern Drake Passage between the SAF and PF. This contrasts with the distribution observed along SR1b, downstream of the Shackleton Fracture Zone (SFZ), where mesoscale variance increases to the south. The DRAKE moorings sample both these local maxima in mesoscale variability (Figure 3, bottom right).

[89] A geostrophic stream function estimated from objective analysis of the mean ADCP currents and altimetry [*Lenn et al.*, 2008] improves on the resolution of the ACC fronts observed in recent climatologies [*Maximenko and Niiler*, 2005; *Olbers et al.*, 1992]. Although the means are from different time periods (Figure 17), interannual variability estimated from differences in mean sea level anomalies for the respective periods do not account for the differences [*Lenn et al.*, 2008]. A total height change of about 140 cm across the ACC is comparable between the ADCP-based mean stream function and the highest-resolution climatology examined [*Maximenko and Niiler*, 2005]. However, the ADCP stream function better resolves the banded structure of the ACC, with narrower jets associated with the ACC fronts separated by quiescent zones of much weaker flow (Figure 17). Using the ADCP stream function together with sea level anomalies, distinct streamlines associated with particular ACC fronts can be identified and are tracked in time-dependent maps of dynamic height [*Lenn et al.*, 2008]. Varying degrees of topographic control can be observed in the preferred paths of the mean fronts through Drake Passage. These streamlines define a natural coordinate system for the ACC in Drake Passage.

4.1.2. Seasonal to Interannual Variability of Temperature

[90] One-time hydrographic CTD transects, such as undertaken during WOCE, provide snapshots of the top-to-bottom mass and property transports. In the eddy-populated Southern Ocean, however, there are questions regarding the representativeness of single hydrographic sections with station spacing of ~50 km for estimation of the mean state of the ocean; additionally, they cannot easily be used to address questions of seasonal to interannual variability. In contrast, the broad-scale sampling of the profiling float array has provided information on the long-term changing heat content of the Southern Ocean [*Gille*, 2002, 2008], but these data do not adequately sample the strong jets, fronts and eddies that require finer resolution. The high-resolution XBT-XCTD sampling is a hybrid of these sampling strategies, with an eddy-resolving station spacing of O (5–15 km) and a short crossing time (2.5 days) making the survey closer to a true snapshot. Beyond single transects, the Drake Passage XBT-XCTD program samples in the time domain. The long-term, spatially coherent nature of the XBT-XCTD sampling program enables detailed studies of statistics, structures and features in the seasonal to interannual variability of the upper ocean water masses in Drake Passage that are not possible using other sampling modes.
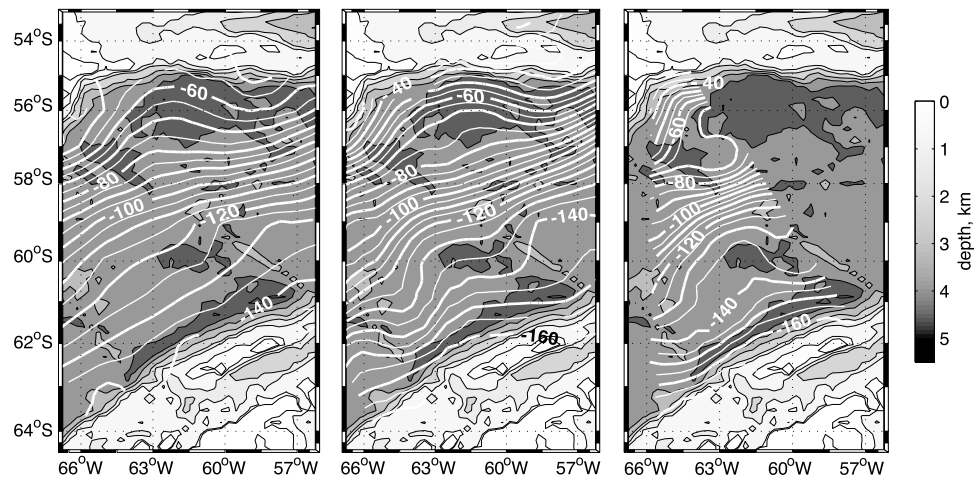
Figure 17. Streamlines (white) correspond to surface height; contour interval is 5 cm. Streamlines from (left) the Southern Ocean atlas dynamic topography relative to 2500 m [*Olbers et al.*, 1992], (middle) the mean dynamic ocean topography of *Maximenko and Niiler* [2005], and (right) stream function derived from the objectively mapped ADCP mean currents by *Lenn et al.* [2008]. Bathymetry is shown in gray scale with contours (black) drawn at 500 m intervals starting at 0 m (adapted from *Lenn et al.* [2008]).

[91] The relatively dense sampling of the XBT transect was designed to capture the mesoscale features and frontal systems in Drake Passage. The position of the PF defined as the northern extent of the 2°C isotherm at 200 m depth [*Botnikov*, 1963] is also associated with a strong velocity jet and a large increase in surface (0–250 m) transport [*Lenn et al.*, 2007]. The sharp temperature gradient across the PF is frequently resolved within just 2–3 XBT profiles. The PF has the strongest temporal variability within Drake Passage with a standard deviation of ~2°C in the upper 75 m of Drake Passage and is generally located between 58°S and 59°S (Figure 18). The closely spaced XBT profiles show the isotherms are near vertical in the PF from the surface to ~300 m depth during austral winter but weaken in summer because of surface heating. South of the PF, cold (<0°C) AASW is found in the upper 150 m during winter, and is capped by surface heating in spring and summer that traps a well-defined temperature minimum layer. Below the AASW lies the upper CDW that is characterized by temperatures of ~2°C and is strongly homogenous, although there is a weak temperature maximum found at ~400–600 m depth. The upper CDW has the lowest-temperature variability of all water masses found in the Drake Passage XBT sections (Figure 18). The largest temperature variability occurs north of the PF, and is associated with mesoscale variations from meanders and eddies. In this region of Drake Passage, eddies are predominantly found north of the PF [*Sprintall*, 2003], and estimates of EKE from the direct ADCP velocity measurements and altimetry are elevated there [*Lenn et al.*, 2007].

[92] Distinct differences are also found north and south of the PF in long-term trends and interannual variability of the upper ocean temperature from 1969 to 2004 in Drake Passage [*Sprintall*, 2008]. North of the PF, statistically significant warming trends of ~0.02°C yr^{-1} are observed that are largely depth independent between 100 and 700 m. A statistically

significant cooling trend of −0.07°C yr^{-1} is observed at the surface south of the PF, which is smaller (−0.04°C yr^{-1}) but still significant when possible seasonal sampling biases are accounted for. The observed annual temperature anomalies are highly correlated with variability in sea ice, and also with the SAM and ENSO climate indices. The temperature trends are largely consistent with a poleward shift of the PF due to a strengthening and southward shift of the westerly winds in the Southern Ocean, which is shown by models to be associated with the increasing positive polarity of the SAM [*Hall and Visbeck*, 2002; *Oke and England*, 2004; *Thompson and Solomon*, 2002]. In the work by *Sprintall* [2008], a complete 36 year time series of the PF position in Drake Passage was not sufficiently well resolved, primarily because the available individual data from the historical archives were not necessarily part of a complete transect across the passage. In addition, the coarser ~50 km station spacing of the historical transects made the determination of the PF problematic. However, the time series of the PF location determined from 13 years of the high-resolution Drake Passage XBT temperature measurements suggests a poleward trend of ~40 km decade^{-1}, consistent with that suggested by the models. No significant trend is evident in the SAF, which in Drake Passage is located in the very north of the passage. We note here the apparent conflict with the results from the WOCE SR1b CTD stations, which indicate a bipolar position of the PF at that line and no significant trend in its position (see section 3) (King and Jullion, manuscript in preparation, 2011). The SR1b results are independent of which definition of PF location is used (transport maximum or thermohaline criterion), thus, the apparent difference cannot be due to different concepts of what determines the PF. Consequently, it appears most likely that the different locations of the sections are responsible, with the SR1b CTD stations being conducted further east in Drake Passage compared with the XBT transects. It is possible that
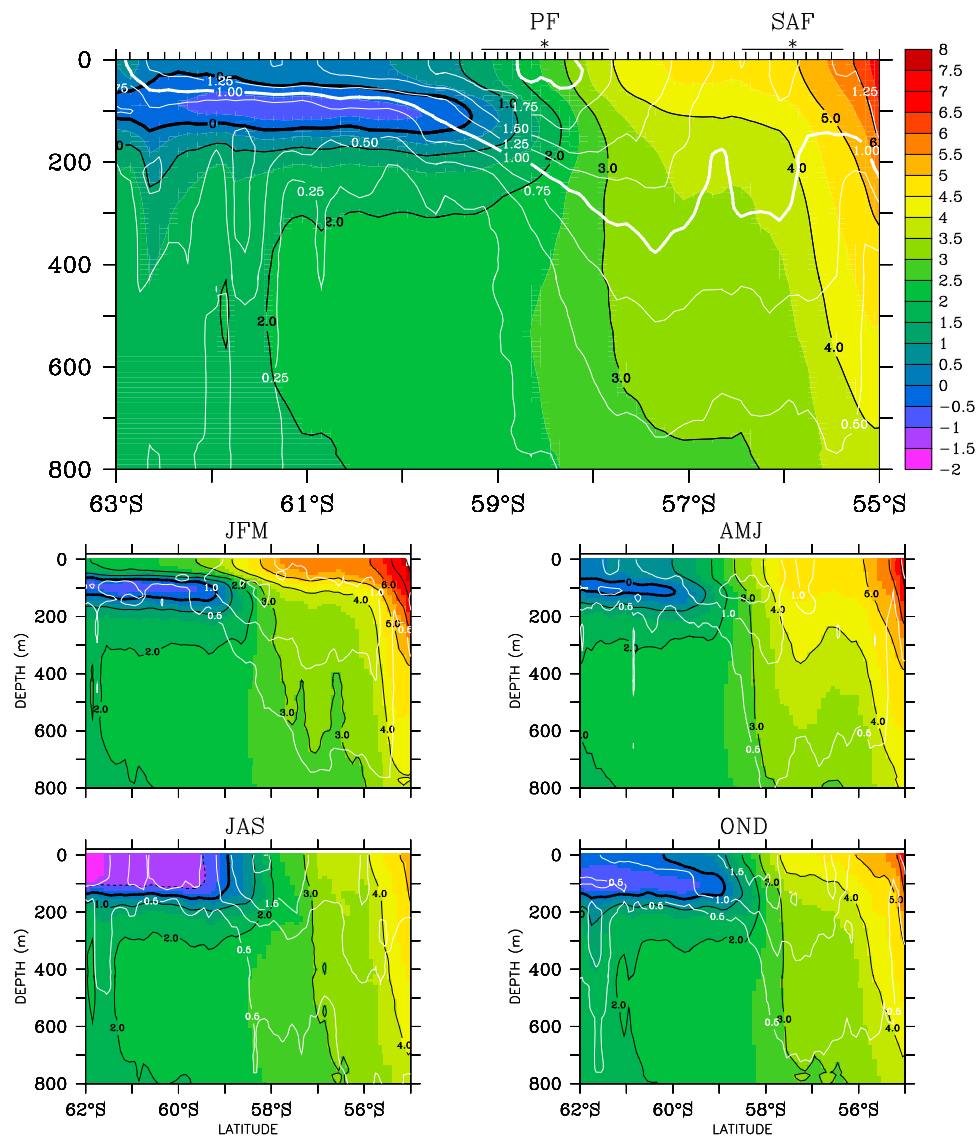
Figure 18. (top) Mean (color) and standard deviation (white contours) of temperature from 90 Drake Passage XBT transects. Typical XBT drop locations are shown on the upper axis. Same data is given as in upper panel but for (middle) January–June and (bottom) July–December.

topographic effects play a role in constraining the location of the PF on SR1b, lying as it does just east of the Shackleton Fracture Zone.

4.1.3. Eddy Momentum and Heat Fluxes

[93] Mesoscale eddies are ubiquitous within the Southern Ocean and have long been thought to be the mechanism for fluxing heat poleward while transmitting wind momentum downward through the water column [*Bryden*, 1979; *Johnson and Bryden*, 1989; *Olbers*, 1998]. However, the proposed link between the Southern Ocean momentum balance and overturning circulation, via an interfacial form stress dependent on the eddy heat flux [*Johnson and Bryden*, 1989], has been challenging to assess. Confirmation requires observations of sufficient duration and temporal and spatial resolution so that the divergence of the eddy fluxes can be estimated with statistical significance. While Drake Passage is one of a few Southern Ocean regions in which moored observations have yielded consistently poleward eddy heat flux estimates,

these vary widely with depth and are sensitive to the record length used [*Bryden*, 1979; *Johnson and Bryden*, 1989; *Sciremammano*, 1979]. An ISOS-inferred interfacial form stress suggested a downward transfer of momentum that exceeded the surface wind stress in Drake Passage [*Johnson and Bryden*, 1989]. South of Tasmania, where other moored observations have provided the necessary vertical resolution, the interfacial form stress was found to be of roughly equal magnitude to the surface wind stress [*Phillips and Rintoul*, 2000]. Estimates of eddy momentum fluxes have likewise proved spatially inhomogeneous, resulting in small lateral gradients of varying sign [*Gille*, 2003; *Hughes and Ash*, 2001; *Morrow et al.*, 1994].

[94] The long-term nature and high spatial resolution of the XBT-ADCP sampling enables an evaluation of the contribution of the eddy momentum and heat fluxes to the ACC momentum balance in the upper 250 m of Drake Passage. Using 7 years of observations, *Lenn et al.* [2011] averaged

gridded eddy flux estimates along mean ACC streamlines to form time mean vertical cross-stream sections of eddy momentum and heat fluxes. Statistically significant stream-averaged cross-stream eddy momentum fluxes confirm that the eddies exchange momentum with the mean SAF and PF, acting to strengthen and sharpen the fronts over the observed depth range while decelerating the flow in the interfrontal zones. The XBT-ADCP observations resolve large poleward eddy heat fluxes of up to -290 kW m^{-2} in the near-surface layer of the PF and SACCF, exceeding deep moored estimates by an order of magnitude. Interfacial form stress could only be calculated in the SAF. It varied little with depth between 100 (the Ekman depth) and 250 m and was in approximate balance with the surface wind stress. Its vertical divergence, estimated over the depth range 100–250 m, was about an order of magnitude greater than the eddy momentum forcing.

4.1.4. Characteristics of the Southern Ocean Ekman Layer

[95] Wind-driven Ekman currents have been difficult to observe directly because, even when forced by strong winds as in the Southern Ocean, their magnitudes are small compared to the background geostrophic circulation. Therefore, despite their importance, Ekman currents are usually inferred from the wind using classical Ekman theory. Without direct measurement of the vertical profile of Ekman currents, accurate predictions of the Ekman layer depth, mean temperature, eddy viscosity and associated Ekman layer heat fluxes cannot be made. In Drake Passage, repeated upper ocean current profiling has resolved the characteristics of the mean Ekman layer [*Lenn and Chereskin*, 2009]. Mean Ekman currents decay in amplitude and rotate anticyclonically with depth, penetrating to 100 m, above the base of the annual mean mixed layer at 120 m. Transport estimated from the observed currents is mostly equatorward and in good agreement with the Ekman transport computed from wind. Since the Ekman layer is shallower than the mixed layer, the mixed layer temperature together with Ekman transport inferred from the wind can be used to estimate the Ekman heat flux contribution to the shallow upper cell of the meridional overturning circulation [*Deacon*, 1937; *Speer et al.*, 2000]. Turbulent eddy viscosities estimated from the time-averaged stress are O (100–1000 m^2 s^{-1}) and decrease in magnitude with depth.

4.1.5. Patterns of Small-Scale Mixing Inferred From XCTDs

[96] Mixing rates in the Southern Ocean remain poorly constrained primarily because few direct observations exist in the region, and this has led to different views concerning how mixing should be incorporated into models of the Southern Ocean meridional circulation. Southern Ocean observational mixing studies have often focused on abyssal mixing processes, and although they clearly show that mixing is intense and widespread, it is characterized by spatial intermittency [e.g., *Heywood et al.*, 2002; *Naveira Garabato et al.*, 2004]. None of these studies have addressed the temporal variability of the mixing events. *Thompson et al.* [2007] used the time series of XCTD temperature and

salinity data collected in Drake Passage to diagnose the mean and seasonal upper ocean diapycnal eddy diffusivities with a view toward understanding what processes dominate upper ocean mixing in the Southern Ocean. Patterns of turbulent diffusivity were inferred from temperature and density inversions using Thorpe-scale techniques [*Dillon*, 1982] and independently from vertical strain spectra. As for other properties in Drake Passage, the PF separates two dynamically different regions. In the upper 400 m, turbulent diffusivities are higher north of the PF (of order 10^{-3} m^2 s^{-1}) compared with south of the PF (of order 10^{-4} m^2 s^{-1} or smaller), and this meridional pattern corresponds to local maxima and minima in both wind stress and wind stress variance [*Thompson et al.*, 2007]. The near-surface diffusivities are also larger during winter months north of the PF. Below 400 m, diffusivities typically exceed 10^{-4} m^2 s^{-1}. Diffusivities decay weakly with depth north of the PF, whereas south of the PF diffusivities increase with depth and peak near the local temperature maximum. *Thompson et al.* [2007] suggest wind-driven near-inertial waves, strong mesoscale activity and double-diffusive convection as possible mechanisms that could give rise to these elevated mixing rates and the observed spatial patterns.

4.1.6. Seasonal to Interannual Variability of ADCP Backscatter

[97] Evidence suggests that the west Antarctic Peninsula region has warmed every decade for the last half century, affecting populations from penguins to krill [*Loeb et al.*, 1997; *Meredith and King*, 2005; *Schofield et al.*, 2010]. Monitoring Antarctic krill distribution is of particular interest since krill are a major source of food for higher predators, and their dominance represents a potential source of instability in the ecosystem. Intensive sampling of zooplankton assemblages in Drake Passage has thus focused on krill spawning habitat, located primarily in the coastal waters adjacent to the Antarctic Peninsula and South Shetland Islands, with sampling limited to the ice-free spring and summer months [e.g., *Hewitt et al.*, 2003]. North of the SACCF, the Discovery Expeditions [*Mackintosh*, 1934] remain the best comprehensive reference for zooplankton taxa throughout much of Drake Passage.

[98] Quantifying krill populations is challenging because of patchiness in their spatial distribution. The ADCP backscatter, while not calibrated absolutely, has been shown to be strongly correlated with the biomass of planktivores [e.g., *Zhou et al.*, 1994]. While the ADCP backscatter amplitude is not calibrated against net tows, it is calibrated from bottom echoes along a repeated transect of the Patagonian shelf. The long-term and highly spatially resolved nature of the ADCP sampling provides a valuable estimate of the space-time variability of backscatter and inferred biomass [*Chereskin and Tarling*, 2007]. Depth-averaged backscatter strength shows a well-defined seasonal cycle, with a peak in summer and a trough in winter, consistent with seasonal changes in planktivore populations. The time series resolves interannual variations in spring transition that can be aliased by seasonal sampling. There is a trend in backscatter strength across the PF, with higher values in northern Drake
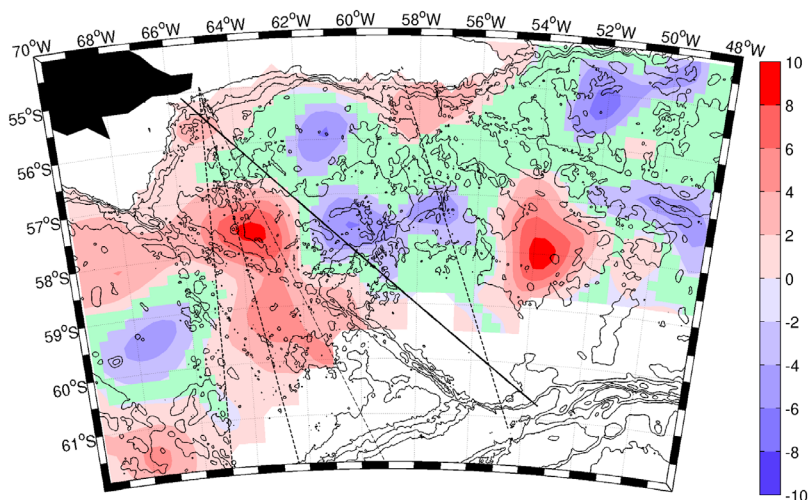
Figure 19. Linear trends in dynamic topography (mm yr^{-1}) from January 1993 to December 2009. The significance of the trend was computed using a two-sided student t-test with a confidence limit of 99%. Areas where the trend is not significant are colored in green. White areas correspond to the regions where the time series are incomplete, and the data from over the continental slope (depth less than 500 m) are disregarded. Black contours represent the bathymetry between 4000 and 1000 m with contour intervals of 500 m. The black diagonal line indicates Jason track 104. Black dashed lines represent repeat XBT-ADCP tracks from the U.S. Antarctic supply vessel (west of track 104) and the repeat hydrographic section SR1b (east of track 104) (updated from *Barré et al.* [2011]).

Passage, in agreement with patterns observed in net tows of the Discovery Expedition [*Mackintosh*, 1934]. South of the SACCF, both planktivores and backscatter have declined over a 6 year period (1999–2006), coincident with a decline in the populations of planktivorous higher predators (e.g., Adelie penguins) in nearby islands [*Forcada et al.*, 2006]. The backscatter time series provides a useful guideline for future, dedicated studies examining the response of the zooplankton community to recent warming trends in the surface waters of this region as well as the changing ice dynamics [*Vaughan et al.*, 2003].

4.2. The DRAKE Project

4.2.1. Experimental Aims and Design

[99] The DRAKE project is a recently concluded experiment consisting of in situ measurements made over a period of about 3 years (February 2006 to April 2009), which are tightly coupled to satellite altimetry (TOPEX/POSEIDON and Jason-1). The measurement array consisted of 10 subsurface current meter moorings deployed below Jason track 104, with individual moorings located at altimeter crossover points (Figure 3, bottom right). A total of 5 full-depth hydrographic sections were occupied on the R/V *Polarstern* cruises that serviced the moorings [*Provost et al.*, 2011]. Early results from analyses of satellite data and the hydrographic data are summarized section 4.2.2, while the time series from the moorings are still preliminary.

4.2.2. Early DRAKE Results

[100] Altimetric time series were used to document the long-term trends in sea surface height, the recurrence of major frontal meanders and statistical links between them [*Barré et al.*, 2011]. Trends are not homogeneous in Drake Passage; for example, a strong positive trend between the

Phoenix Antarctic Ridge (PAR) and the Shackleton Fracture Zone is consistent with a southward shift of the PF there, in agreement with the observations along the XBT-ADCP repeat tracks (Figure 19). The trend changes sign in the adjacent Yaghan Basin, however, suggesting a regional effect caused by the complicated bathymetry and geometry. Topography favors the recurrence of some meanders and eddies in specific spots in Drake Passage. For example, a dipole occurring with a close to annual periodicity is observed at the entrance to Drake Passage over the PAR and corresponds to adjacent meanders of the SAF and PF [*Barré et al.*, 2011] (Figure 20). An anticyclonic meander of the PF was found to recur over the Ona seafloor depression to the northwest of the Ona Basin (54°W, 58°S) and constitutes an important element of the cyclonic recirculation in the Ona Basin [*Barré et al.*, 2008].

[101] *Barré et al.* [2011] used isolines of absolute dynamic topography from satellite altimetry data to map out locations of fronts and eddies, providing a temporal and spatial context for the 2006 DRAKE mooring deployment cruise (ANT-XXIII/3, January–February 2006). Eight fronts were identified from local maxima in SSH gradients and associated with SSH values. Consistent with *Lenn et al.* [2008], the multiple branches of the ACC fronts were observed to merge into single jets in the narrowest part of the passage, with two branches of the SAF merging at about 61°W and three branches of the PF merging over the SFZ. The SACCF branches could also be traced using altimetry, and a remarkable agreement was found between the location of the frontal branches and eddies detected by altimetry and the patterns observed in sea surface temperature and ocean color. The crest of the SFZ was found to constitute a barrier in the south of Drake Passage, causing the two SACCF
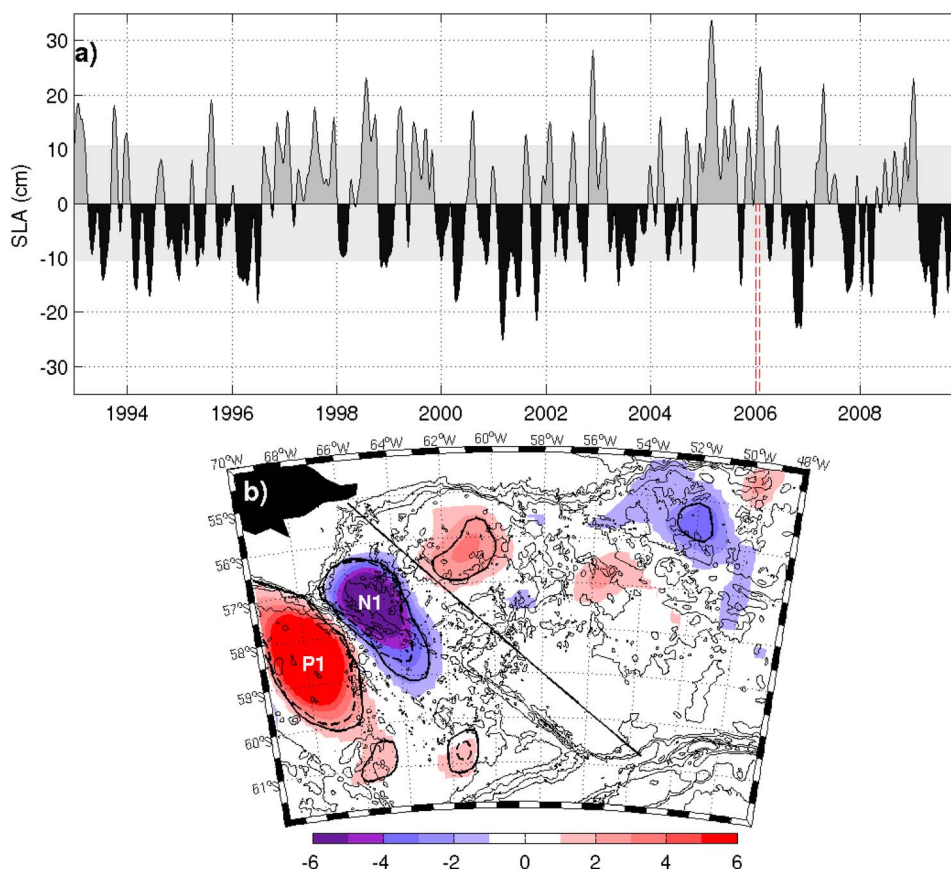
Figure 20. (a) Time series of sea level anomaly (SLA) over a 1° × 1° box centered at 68°W and 58.5°S (location P1). The linear trend has been removed. The gray shading represents one standard deviation. (b) Regression of SLA, in Drake Passage, on the normalized time series in Figure 3a. Solid black contours represent the correlation at the 90% confidence level, and dashed black contours represent the 95% confidence level. The regression map suggests that the strong anomaly (P1) on the western side of the PAR can be associated with an anomaly of the opposite sign (N1) on the eastern side of the PAR. Thin black lines are bathymetry isobaths (2000, 3000, and 4000 m) (updated from *Barré et al.* [2011]).

branches to separate by about 400 km, and creating sheltered conditions in partial isolation from the ACC, while promoting an active recirculation region in the Ona Basin. This recirculation, marked by cyclonic eddies carrying cold, fresh and oxygenated water from south of the Southern Boundary of the ACC, causes effective ventilation of the whole CDW density range [*Provost et al.*, 2011].

[102] In 2006 a highly resolved (20 km station spacing) hydrographic Lowered Acoustic Doppler Current Profiler (LADCP) section under Jason track 104 was occupied twice within 3 weeks, providing a unique opportunity to document full depth in situ variability at about a 10 day interval. Between the two occupations, the contributions of frontal meanders and eddies to the total volume transport changed notably, although the net transport changed by only 10% and agreed within confidence limits with prior WOCE and ISOS estimates [*Renault et al.*, 2011]. Encouragingly, estimates of total transport by two different methods agreed within errors: A mean estimate of transport for the repeated section computed from LADCP observations was 142 ± 9.7 Sv, in good agreement with 133 ± 7 Sv estimated from

geostrophic velocities referenced to full-depth LADCP profiles via least squares.

[103] Considerable differences in properties between the 10 day-apart sections are observed throughout the whole water column with values as high as 0.2°C in temperature, 0.01 in salinity, 0.03 kg m^{-3} in neutral density, and 10 μmol kg^{-1} in dissolved-oxygen concentration found below a depth of 3000 m [*Provost et al.*, 2011; *Sudre et al.*, 2011]. Only part of the difference is attributable to frontal or eddy displacements along the section. The other part results from the spatial heterogeneity of water properties upstream of the section and the funneling of the flow due to the topographic constraints of the SFZ. The considerable short-term differences in water properties in rather large-scale structures that cannot be accounted for by frontal motions along the section points to the need for highly resolved measurements in both time and space in order to avoid aliasing.

4.3. The cDrake Experiment

4.3.1. Experimental Aims and Design

[104] cDrake is a field experiment to resolve the seasonal to interannual variability of the ACC transport and dynamics

over a 4 year period using bottom-moored Current and Pressure-Recording Inverted Echo Sounders (CPIES). The cDrake array (Figure 3, bottom right) comprises a transport line of 21 CPIES spanning 800 km across the passage, and a local dynamics array (LDA) of 21 CPIES spanning 120 km cross stream and 240 km downstream. The LDA is situated where surface variability observed by altimetry and ship-board ADCP is a local maximum [*Lenn et al.*, 2007]. The goal for the transport line is to determine the time-varying total ACC transport, its vertical structure partitioned between barotropic and baroclinic components and its lateral structure partitioned among the multiple ACC jets. The goal for the LDA is to make 4-D stream function maps with meso-scale resolution in order to quantify the vertical transport of momentum in the ACC from the surface to the seafloor, to describe the mesoscale eddy field and to quantify eddy/mean-flow interactions. The cDrake array was deployed during the 2007–2008 International Polar Year. Data are collected annually by acoustic telemetry to a ship, and instrument recovery is planned for late 2011.

[105] The pressure-recording inverted echo sounder (PIES) moored on the seafloor measures bottom pressure and emits sound pulses to measure the round-trip travel times of these pulses to the sea surface and back (τ). The CPIES includes a Doppler current sensor tethered 50 m above it to measure the near-bottom current outside the benthic boundary layer. The instrument internally processes data using typical post-processing techniques and saves a daily mean value to a file that resides in the instrument. Internal processing of pressure and current data ensures that tides are not aliased. Results described here are based primarily on telemetered data and, when available, from the recovered records of instruments that required replacement.

[106] Measurements of τ from the IES are used to estimate full water column profiles of temperature, salinity and density. These profiles are on the basis of historical hydrography for the region, from which an empirical lookup table (the so-called gravest empirical mode (GEM)) is established to use as an index for vertical profiles of temperature, salinity, and density. Through geostrophy, laterally separated pairs of these density profiles yield vertical profiles of baroclinic velocity. The deep pressure and current measurements provide the reference velocity to render the velocity profiles absolute. Deep pressures are leveled by adjusting records to the same geopotential surface under the assumption that long-time averages of near bottom currents and bottom pressures are in geostrophic balance. These methods have been successful in many regions, including the ACC [*Meinen et al.*, 2003; *Watts et al.*, 2001].

4.3.2. Early cDrake Results

[107] The first year of daily averaged currents measured at 50 m above bottom revealed extremely large mean velocities in northern Drake Passage, exceeding 10 cm s^{-1} at 15 sites north of the PF, with mean directions that were not aligned with the surface fronts (Figure 21) [*Chereskin et al.*, 2009]. The large bottom currents suggest that bottom friction may play a more significant role in the ACC momentum balance than previously thought, at least locally.

Topographic steering was most evident at the continental margins. Deep EKE was maximum at about 200 cm^2 s^{-2} between the SAF and PF, coinciding with the location, but about one quarter of the value, of a maximum in surface EKE [*Chereskin et al.*, 2009]. The LDA observations showed multiple high-speed current events, with peak speeds of 60–70 cm s^{-1} and lasting 30–70 days, that were coherent across sites separated by 45 km. These events corresponded to the spinup of deep eddies coinciding with meanders in the surface fronts, consistent with deep cyclogenesis (Figure 21). A longer 2 year record is consistent with the first year results.

[108] Two year bottom pressure variance within the LDA was two times higher than variance to the north and three times higher than variance to the south (K. A. Donohue et al., Barotropic transport variability in Drake Passage from the cDrake experiment, manuscript in preparation, 2011). Bottom pressure in the LDA was strongly influenced by the meandering of the two northern ACC fronts. Transport was sensitive to the choice of endpoints, particularly the northern endpoint. A suite of reasonable calculations yielded barotropic transport variability with standard deviations near 10 Sv. In all cases, large transport fluctuations, as high as 30 Sv, occurred over time scales of weeks to days. Ultimately a multiple-site average reduced local small-scale eddy variability at both the southern and northern end points and best described barotropic transport in Drake Passage. Neither time series by itself captured all the transport variability across the Passage. Within the frequency band 1/200–1/3 d^{-1}, the northern (southern) time series explained about 44% (32%) of the variance in transport. This is largely consistent with *Hughes et al.* [2003], who derived a correlation around 0.7 between southside pressure and modeled total transport, indicating that around half the total transport variability could be captured by a single gauge. Coherence between northern and southern time series existed, and the phase relationship changed with frequency. To focus on large-scale bottom pressure variability, empirical orthogonal functions were calculated for frequencies greater than 1/200 d^{-1} within four bands. Two transport modes were identified that both correlated with the Antarctic Oscillation Index. In the 12–8 day band, a transport mode with spatial decay of 1/800 km^{-1} existed with northern sites in phase with southern sites. In the 40–12 day band, a passage-wide transport mode has northern sites out of phase with southern sites. The broad scale of both modes suggests that in Drake Passage the southern Antarctic transport mode exists along f/H contours that are both blocked and unblocked.

[109] The cDrake pressure and IES measurements show the relative contributions of the mass-loading and steric constituents of sea surface height anomaly (SSHA). Round-trip travel time measurements were converted to geopotential using historical hydrography [*Cutting*, 2010]. Geopotential was then divided by gravity to determine the steric component of SSHA. The mass-loading component of SSHA was computed by dividing the bottom pressure anomaly by the product of density and local gravity. In Drake Passage, the mass-loading and steric SSHA components are uncorrelated,
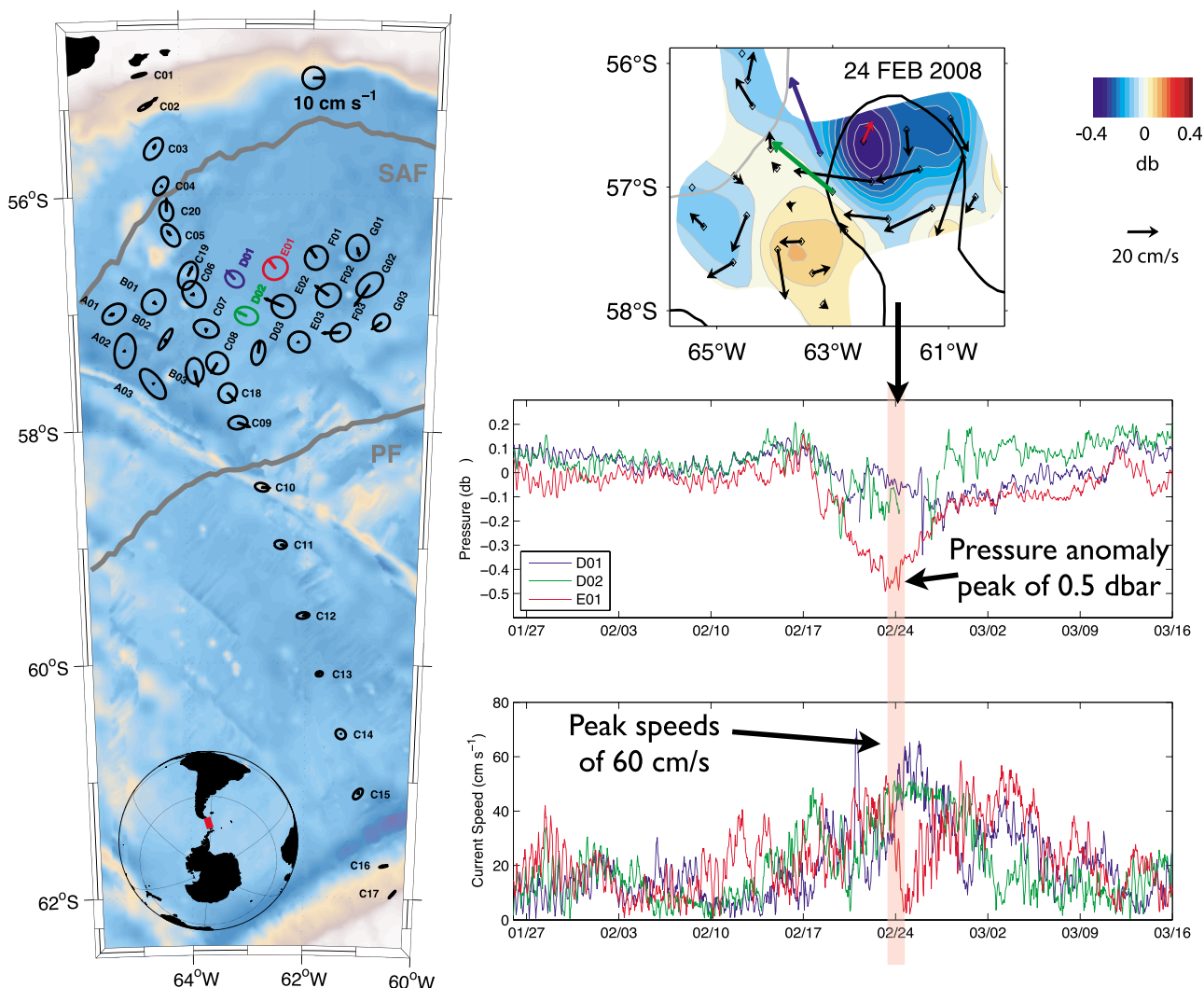
Figure 21. cDrake bottom currents and pressures. (left) Record length (1 year) means and standard deviation ellipses for currents observed 50 m above bottom. Fifteen sites have means in excess of 10 cm s^{-1}, all in northern Drake Passage. Mean directions do not, in general, coincide with the mean fronts, shown here as gray lines from the *Lenn et al.* [2008] streamline analysis. (bottom right) Time series for three sites during the most energetic cyclogenesis event (there were about five in a year) show a peak pressure anomaly of 0.5 dbar; currents peak at 60 cm s^{-1}. (top right) Pressure anomaly (dbar, color) where blues are low pressure and daily mean currents on 24 February 2008, when a deep cyclone center was near site E01 (adapted from *Chereskin et al.* [2009]).

except in the LDA at times when strong cyclogenesis occurs. Relative contributions of steric and mass-loading components varied along the transport line. North of 57°S, steric SSHA variance exceeded 60% of the total SSHA variance. South of 59°S, the mass-loading SSHA variance exceeded 40% of the total SSHA variance and in places reached 65% of the total variance. CPIES SSHA complements altimetric SSHA in several ways. First, the time series can quantify the aliasing of the SSHA signal from satellite altimeters. On the basis of the first year of cDrake estimates, the near 10 day repeat sampling (e.g., TOPEX/POSEIDON, Jason-1, and Jason-2) likely leads to aliased variance that exceeds 20% of the total signal variance within the LDA and on the southern end of the transport line south of 58°S. Second, bottom pressure data contributes to the validation of numerical models used to reduce the aliased variance in the altimeter SSHA data set.

4.3.3. Ongoing cDrake Investigations

[110] CPIES are an integrating measurement technique and offer a complementary view to point current meter observations such as those made during ISOS and DRAKE. While point current meters have poor vertical resolution, CPIES are limited to geostrophic and barotropic velocities, so future work to combine contemporaneous cDrake and DRAKE observations during their overlap measurement period should yield a more complete description of the vertical and horizontal structure of the ACC through exploitation of the different sampling strengths.

[111] cDrake observations will be used to assess aliasing in ongoing time series (e.g., altimetry, XBTs) and to guide future monitoring systems. The cDrake observations will also provide metrics for model validation. cDrake observations will be assimilated in the Southern Ocean State Estimate (SOSE) [*Mazloff et al.*, 2010]. The initial fit of the observations with the SOSE solution will provide information as to the uncertainty of dynamical estimates drawn from the state estimate. In return, the SOSE will provide a framework for dynamic interpolation useful in interpreting the observations.

4.4. The DIMES Experiment

[112] The Diapycnal and Isopycnal Mixing Experiment in the Southern Ocean (DIMES) is an international (United Kingdom and United States), multicruise experiment seeking to obtain the first systematic measurements of mixing processes in two contrasting regimes (the Southeast Pacific and Southwest Atlantic) of the ACC centered around Drake Passage. The project is motivated by the perceived acute sensitivity of the oceanic overturning circulation and a range of important features of the wider climate system to the representation of mixing processes in the Southern Ocean, and by the existence of seemingly conflicting observational clues on the character and controlling dynamics of diapycnal and isopycnal mixing in the region. For example, whereas much of the theoretical work on understanding the Southern Ocean overturning assumes weak diabaticity below the surface mixed layer [e.g., *Marshall and Radko*, 2003, 2006], intense turbulent mixing has been suggested to occur because of the breaking of internal waves generated by ACC flow over small-scale topography [*Naveira Garabato et al.*, 2004, 2007; *Nikurashin and Ferrari*, 2010]. Similarly, the structure of eddy-induced isopycnal stirring in the Southern Ocean remains a matter of debate, with analyses of various numerical models and observations suggesting that while it is generally reduced at the core of the eddy-rich ACC jets [e.g., *Smith and Marshall*, 2009; *Abernathey et al.*, 2010; *Ferrari and Nikurashin*, 2010; *Naveira Garabato et al.*, 2011], it is enhanced at selected sites in the vicinity of topography [e.g., *Naveira Garabato et al.*, 2011] for reasons that are poorly understood at present.

[113] In order to achieve this overarching goal, DIMES investigators are presently in the course of obtaining multiple, concurrent measures of the rates of isopycnal and diapycnal mixing and upwelling, and their underpinning physical processes, throughout the study region. The focal element of the experiment is the spreading of a chemical tracer (trifluoromethyl sulphur pentafluoride, CF_3SF_5) that was released in the upper CDW layer of the SE Pacific zone of the ACC in January–February 2009, with which the spatially and temporally averaged rates of middepth mixing and upwelling throughout the experimental domain are being assessed. In order to measure diapycnal mixing at other depths and investigate the physical processes driving it, full-depth profiles of oceanic microstructure are being collected with three different free-falling profilers during five further austral summer cruises, and fine structure pro-

files obtained year-round with EM-APEX floats within and above the tracer cloud. Isopycnal stirring by mesoscale eddies is also being measured at two different vertical levels by monitoring the dispersion of isopycnal RAFOS floats deployed in clusters at various stages of the experiment and tracked acoustically using moored sound sources. The dynamics regulating the coupling between mesoscale eddies and internal waves are being studied with a sub-mesoscale cluster of 6 moorings deployed in eastern Drake Passage between December 2009 and January 2012. This portfolio of observations is being complemented by a range of inverse and numerical modeling efforts that seek to optimize the methodology of the observational analyses, investigate the controlling dynamics of the mixing processes under scrutiny, and assess the sensitivity of large-scale overturning to those processes. The initial results of the DIMES fieldwork reveal that the Southeast Pacific sector hosts remarkably weak turbulent diapycnal mixing at middepth [*Ledwell et al.*, 2011]. The fieldwork phase of the experiment is due to conclude in the austral summer of 2013–2014.

5. DISCUSSION AND CONCLUSIONS

[114] Because of its long history of sustained measurements, Drake Passage is the best-observed region of the Southern Ocean, and arguably the best understood. Indeed, it stands as one of the most comprehensively monitored continent-to-continent sections in the world. Scientific progress here since the early hydrographic sections and the days of ISOS has been profound. In particular, the sustained nature of the measurement programs at Drake Passage has enabled some particular insights to be made that would not have been possible without such targeted, long-term measurements. These include (but are certainly not limited to) the following:

[115] 1. Quantification of the transport fluctuations at subannual periods, leading to an understanding of the wind forcing of such fluctuations and their dynamical interaction with topography.

[116] 2. A realization that the ACC transport is remarkably steady on interannual and longer time scales relative to much larger proportional changes in the overlying winds, and a growing understanding of the mesoscale processes and feedbacks responsible for this.

[117] 3. Recognition of the role of coupled climate modes in dictating the horizontal transport, and the role of anthropogenic processes in this.

[118] 4. Identification of changes in properties of water masses relevant to both the upper and lower limbs of the overturning circulation in the Southern Ocean, and an understanding of the dynamics and climatic processes responsible for these, as well as their impacts.

[119] 5. Realization of the pivotal role of Southern Ocean eddies in setting the ACC transport through Drake Passage, the residual overturning circulation across the ACC, and the global stratification.

[120] The sustained monitoring programs that generated these advances in understanding of the Southern Ocean almost all chose Drake Passage primarily for logistical

reasons, it being the narrowest section that captures all of the ACC, and also a trade route for many vessels traveling to and from the most populated part of Antarctica. However, it is noteworthy that most of the major findings to have come from Drake Passage monitoring have applicability and implications that extend well beyond providing a baseline understanding of the oceanography of the Passage itself. For example, elucidation of the dynamics behind the transport fluctuations is relevant to the ACC in all sectors of the Southern Ocean, while the changes in the Southern Ocean overturning observed at Drake Passage have implications for regional and even global climate via processes such as the drawdown of anthropogenic carbon from the atmosphere. There is an implicit criterion here, of producing results that have a significance that transcends the location of the measurements, that is, in many ways, a critical test of the value of a sustained monitoring program. In this context, and against the background of what has been learned at Drake Passage over the past several decades, it is worth asking whether the monitoring efforts here should be continued, and if so why and how.

[121] With regard to determining the horizontal flow through Drake Passage and its variability, a devil's advocate might claim that this task has almost been completed. In particular, given that the long-term transport appears to have been remarkably stable, with changes in flow of around 5% of the mean on interannual time scales despite much larger relative changes in wind stress, the argument could be advanced that future changes in transport are also likely to be small (howsoever one defines "small"), and thus the need to monitor them is less compelling. This argument is perhaps not without some merit, however, the counterpoint is that the dynamics that control the transport variability on interannual and longer periods (and that are responsible for it being small) are still imperfectly known. For example, the feedbacks between the mean flow, eddies and topography that generate the observed lag between transport changes, and changes in eddy intensity is a topic deserving of further investigation. Coarse resolution coupled climate models represent such processes only very crudely, and if their depictions of the Southern Ocean are to be improved, there is a need to improve dynamical understanding, and to test this understanding with observations.

[122] A related point that should be made is that the previously recognized low level of transport variability on interannual and decadal time scales does not, in fact, necessarily imply that future changes will be equally small. In an inherently nonlinear system, there is the possibility of moving to a different dynamical regime, where horizontal flow responds differently to forcing. For example, if it is accepted that the ACC is currently close to an eddy-saturated state (where transport varies little with respect to winds, but eddy intensity changes more), there is a question concerning what will happen if the wind strength reduces significantly in future decades. Such a decrease in wind is conceivable as recovery from the ozone hole progresses, and is predicted by a number of climate models that include stratospheric ozone processes.

[123] A further driver for sustaining the monitoring of the flow at Drake Passage is that the measurements are increasingly seen as being key in the design of a system for monitoring the overturning circulation in the South Atlantic (see http://www.aoml.noaa.gov/phod/SAMOC/for details on the South Atlantic Meridional Overturning Circulation initiative). In this context, the Drake Passage data provide the boundary conditions for fluxes entering the Atlantic via the cold water path. SAMOC aims to monitor both this and the corresponding warm water path fluxes as functions of time, as well as their impacts on the meridional overturning and gyre circulations in the South Atlantic. This is also strongly connected with the emerging SOOS, which includes a focus on ocean circulation and its role in climate, and also on the need for sustained interdisciplinary measurements in the Southern Ocean in response to a variety of strategic drivers.

[124] While Drake Passage monitoring was largely initiated to elucidate the characteristics of the horizontal flow, numerous other important findings have emerged from the data sets collected to date. Perhaps the most significant among these is the recognition of changes in properties in both the upper and lower limbs of the Southern Ocean overturning, for example, changes in the AAIW and SAMW temperatures and salinities at the location where these water masses enter the Atlantic, and changes in the AABW properties as this water mass exits the Weddell Sea to become the abyssal layer of the Atlantic circulation. Such changes are increasingly seen to be of global significance: Southern Ocean overturning is a key process in modulating the concentrations of atmospheric CO_2, including the anthropogenic component, and the sequestration of this CO_2 in the region of the ACC is one of the reasons why this area is particularly susceptible to ocean acidification.

[125] Our judgment is thus that continuing the sustained measurements in Drake Passage is important, though increasingly it is the measurements that relate to the three-dimensional circulation of the Southern Ocean (and the dynamical controls thereon), rather than just the horizontal flow, that are seen to be the most compelling strategic drivers. If such monitoring is to be continued, the scientific community must challenge itself to deliver the key measurements in the most strategic, cost-effective and scientifically beneficial way. There is also the need to target the monitoring to be as societally beneficial as possible, to justify its continuation against the pressures of different nations' funding systems.

[126] In terms of a monitoring system capable of meeting these criteria, there are some requirements that are already clearly established. Specifically there is a need for sampling with a frequency that is sufficiently high to avoid aliasing of the short-period variability when trying to determine long-period changes in transport, and there is also a need for internal measurements of the water column from which to infer and attribute changes in overturning. Satellite-based measurements of sea surface height (e.g., the Jason series of altimeters) and of temporal and spatial variations in space gravity (GRACE and GOCE) can add useful information,

but cannot meet the requirements by themselves. In practice, this means that a combination of ship-based hydrographic work and in situ observations from coastal tide gauges, moorings and/or bottom lander systems will be needed for the foreseeable future.

[127] There are aspects of existing and previous Drake Passage monitoring programs that are far from optimal. For example, chemical and biogeochemical tracers have only been measured sporadically on Drake Passage sections, despite routine drawing of water samples for salinity analysis. The Drake Passage monitoring effort should be developed to incorporate some of the more compelling of such measurements, including regular full-depth profiles of carbonate system parameters, dissolved oxygen, and so on.

[128] Further, it is very much the case that the current effort at Drake Passage has evolved rather than being planned. Various nations are contributing very significantly, but their efforts are not especially well-coordinated spatially, nor is there a particularly optimal use of resource (either human or technological). To some extent this is inevitable, and a direct consequence of the opportunistic nature of many of the measurements being made. Nonetheless, improved international strategic oversight and planning would be beneficial in maximizing the usefulness and cost-effectiveness of Drake Passage observations. This should be a key challenge to the newly described SOOS.

[129] It is worth recognizing that the effort currently expended at Drake Passage is close to the maximum that is likely to be sustainable for the future, in terms of both human and technical resources, especially with regard to ship-based hydrography, moorings and bottom landers. If substantially more data are required in the future, for example, to provide the year-round and multiyear coverage needed to resolve the seasonal cycles and interannual variability of key properties such as heat flux, then new strategies and technologies will need to be brought to bear. Profiling floats have revolutionized our ability to obtain near real-time data from the Southern Ocean; however, the strong flow means that such floats tend to pass very rapidly through Drake Passage, and because they move generally parallel to streamlines, they are of limited value for flux calculations. To make substantial progress would require the development and deployment of other new technologies, such as long-duration autonomous underwater vehicles (AUVs) and gliders capable of profiling to the seabed in Drake Passage, and capable of navigating autonomously in regions of rapid flow. Existing technologies such as bottom pressure recorders also need development, such that they provide well-calibrated long-term data sets with minimized drift and minimum requirements for maintenance and refurbishment.

[130] Overall, Drake Passage stands as the region of the harsh, remote Southern Ocean from which the most data and understanding have been obtained. Many of the science drivers for sustained observations here remain strong and relevant, though these are evolving, and the measurements undertaken and the technologies used to obtain them need to evolve in parallel. The challenges are significant, but need to be addressed if the scientific and societal worth of the measurements are to remain demonstrable, and for the monitoring to be sustained into the future.

REFERENCES

Abernathey, R., J. Marshall, M. Mazloff, and E. Shuckburgh (2010), Critical layer enhancement of mesoscale eddy stirring in the Southern Ocean, *J. Phys. Oceanogr.*, *40*(1), 170–184, doi:10.1175/2009JPO4201.1.

Allison, L. C., H. L. Johnson, D. P. Marshall, and D. R. Munday (2010), Where do winds drive the Antarctic Circumpolar Current?, *Geophys. Res. Lett.*, *37*, L12605, doi:10.1029/2010GL043355.

Allison, L. C., H. L. Johnson, and D. P. Marshall (2011), Spin-up and adjustment of the Antarctic Circumpolar Current and global pycnocline, *J. Mar. Res.*, in press.

Angell, J. K., and J. Korshover (1964), Quasi-biennial variations in temperature, total ozone and tropopause height, *J. Atmos. Sci.*, *21*, 479–492, doi:10.1175/1520-0469(1964)021<0479:QBVITT>2.0. CO;2.

Aoki, S. (2002), Coherent sea level response to the Antarctic Oscillation, *Geophys. Res. Lett.*, *29*(20), 1950, doi:10.1029/ 2002GL015733.

Aoki, S., M. Hariyama, H. Mitsudera, H. Sasaki, and Y. Sasai (2007), Formation regions of Subantarctic Mode Water detected by OFES and Argo profiling floats, *Geophys. Res. Lett.*, *34*, L10606, doi:10.1029/2007GL029828.

Barker, P. F. (2001), Scotia Sea regional tectonic evolution: Implications for mantle flow and palaeocirculation, *Earth Sci. Rev.*, *55*, 1–39, doi:10.1016/S0012-8252(01)00055-1.

Barker, P. F., B. Dieckmann, and C. Escutia (2007), Onset of Cenozoic Antarctic glaciation, *Deep Sea Res., Part II*, *54*, 2293–2307, doi:10.1016/j.dsr2.2007.07.027.

Barré, N., C. Provost, N. Sennechael, and J. Hak Lee (2008), Circulation in the Ona Basin, southern Drake Passage, *J. Geophys. Res.*, *113*, C04033, doi:10.1029/2007JC004549.

Barré, N., C. Provost, A. Renault, and N. Sennechael (2011), Fronts, meanders and eddies in Drake Passage during ANT-XXIII/3 cruise in January–February 2006: A satellite perspective, *Deep Sea Res., Part II*, *58*, 2533–2554, doi:10.1016/j.dsr2.2011. 01.003.

Bindoff, N. L., et al. (2007), Observations: Oceanic climate change and sea level, in *Climate Change 2007: The Physical Science Basis: Contribution of Working Group I to the Fourth Assessment Report of the Intergovernmental Panel on Climate Change*, edited by D. Q. S. Solomon et al., pp. 385–432, Cambridge Univ. Press, Cambridge, U. K.

Böning, C. W., A. Dispert, M. Visbeck, S. R. Rintoul, and F. U. Schwarzkopf (2008), The response of the Antarctic Circumpolar Current to recent climate change, *Nat. Geosci.*, *1*, 864–869, doi:10.1038/ngeo362.

Botnikov, V. N. (1963), Geographical position of the Antarctic Convergence Zone in the Southern Ocean, *Sov. Antarct. Exped. Inf. Bull.*, 4, 324–327.

Bryden, H. (1979), Poleward heat flux and conversion of available potential energy in Drake Passage, *J. Mar. Res.*, 37, 1–22.

Bryden, H. L., and R. D. Pillsbury (1977), Variability of the deep flow in Drake Passage from yearlong current measurements, *J. Phys. Oceanogr.*, 7, 803–810, doi:10.1175/1520-0485(1977)007<0803:VODFIT>2.0.CO;2.

Caldeira, K., and P. B. Duffy (2000), The role of the Southern Ocean in uptake and storage of anthropogenic carbon dioxide, *Science*, 287, 620–622, doi:10.1126/science.287.5453.620.

Cartwright, D. E. (1999), *Tides: A Scientific History*, Cambridge Univ. Press, Cambridge, U. K.

Chelton, D. B. (1982), Statistical reliability and the seasonal cycle: Comments on "Bottom pressure measurements across the Antarctic Circumpolar Current and their relation to the wind," *Deep Sea Res., Part A*, 29(11), 1381–1388, doi:10.1016/0198-0149(82)90016-4.

Chereskin, T. K., and G. A. Tarling (2007), Interannual to diurnal variability in the near-surface scattering layer in Drake Passage, *ICES J. Mar. Sci.*, 64, 1617–1626.

Chereskin, T. K., K. A. Donohue, D. R. Watts, K. L. Tracey, Y. L. Firing, and A. L. Cutting (2009), Strong bottom currents and cyclogenesis in Drake Passage, *Geophys. Res. Lett.*, 36, L23602, doi:10.1029/2009GL040940.

Clowes, A. J. (1933), Influence of the Pacific on the circulation in the southwest Atlantic Ocean, *Nature*, 131, 189–191, doi:10.1038/131189a0.

Cunningham, S. A., S. G. Alderson, B. A. King, and M. A. Brandon (2003), Transport and variability of the Antarctic Circumpolar Current in Drake Passage, *J. Geophys. Res.*, 108(C5), 8084, doi:10.1029/2001JC001147.

Cutting, A. L. (2010), *Constituents of Sea Surface Height Variability*, 68 pp., Univ. of R. I., Kingston.

Danabasoglu, G., J. C. McWilliams, and P. R. Gent (1994), The role of mesoscale tracer transports in the global ocean circulation, *Science*, 264, 1123–1126, doi:10.1126/science.264.5162.1123.

Deacon, G. E. R. (1937), *The Hydrology of the Southern Ocean*, 124 pp., Cambridge Univ. Press, Cambridge, U. K.

Dillon, T. M. (1982), Vertical overturns: A comparison of Thorpe and Ozmidov scales, *J. Phys. Oceanogr.*, 87, 9601–9613.

Döös, K., and D. J. Webb (1994), The Deacon cell and the other meridional cells of the Southern Ocean, *J. Phys. Oceanogr.*, 24, 429–442, doi:10.1175/1520-0485(1994)024<0429:TDCATO>2.0.CO;2.

Fahrbach, E., M. Hoppema, G. Rohardt, M. Schröder, and A. Wisotzki (2004), Decadal-scale variations of water mass properties in the deep Weddell Sea, *Ocean Dyn.*, 54, 77–91, doi:10.1007/s10236-003-0082-3.

Fandry, C., and R. D. Pillsbury (1979), On the estimation of absolute geostrophic volume transport applied to the Antarctic Circumpolar Current, *J. Phys. Oceanogr.*, 9, 449–455, doi:10.1175/1520-0485(1979)009<0449:OTEOAG>2.0.CO;2.

Ferrari, R., and M. Nikurashin (2010), Suppression of eddy mixing across jets in the Southern Ocean, *J. Phys. Oceanogr.*, 40, 1501–1519, doi:10.1175/2010JPO4278.1.

Fetter, A. F. H., and R. P. Matano (2008), On the origins of the Malvinas Current in a global, eddy-permitting numerical simulation, *J. Geophys. Res.*, 113, C11018, doi:10.1029/2008JC004875.

Forcada, J., P. N. Trathan, K. Reid, E. J. Murphy, and J. P. Croxall (2006), Contrasting population changes in sympatric penguin species in association with climate warming, *Global Change Biol.*, 12, 411–423, doi:10.1111/j.1365-2486.2006.01108.x.

Foster, L. A. (1972), *Current Measurements in the Drake Passage*, 61 pp., Dalhousie Univ., Halifax, N.S.

FRAM group (1991), An eddy-resolving model of the Southern Ocean, *Eos Trans. AGU*, 76, 169–175.

Fučkar, N. S., and G. K. Vallis (2007), Interhemispheric influence of surface boundary conditions on a circumpolar current, *Geophys. Res. Lett.*, 34, L14605, doi:10.1029/2007GL030379.

Gent, P. R., and J. C. McWilliams (1990), Isopycnal mixing in ocean circulation models, *J. Phys. Oceanogr.*, 20, 150–155, doi:10.1175/1520-0485(1990)020<0150:IMIOCM>2.0.CO;2.

Gent, P. R., J. Willebrand, T. J. McDougall, and J. C. McWilliams (1995), Parameterizing eddy-induced tracer transports in ocean circulation models, *J. Phys. Oceanogr.*, 25, 463–474, doi:10.1175/1520-0485(1995)025<0463:PEITTI>2.0.CO;2.

Gille, S. T. (2002), Warming of the Southern Ocean since the 1950s, *Science*, 295, 1275–1277, doi:10.1126/science.1065863.

Gille, S. T. (2003), Float observations of the Southern Ocean. Part II: Eddy Fluxes, *J. Phys. Oceanogr.*, 33, 1182–1196, doi:10.1175/1520-0485(2003)033<1182:FOOTSO>2.0.CO;2.

Gille, S. T. (2008), Decadal-scale temperature trends in the Southern Hemisphere ocean, *J. Clim.*, 21(18), 4749–4765, doi:10.1175/2008JCLI2131.1.

Gille, S. T., and C. W. Hughes (2001), Aliasing of high-frequency variability by altimetry: Evaluation from bottom pressure recorders, *Geophys. Res. Lett.*, 28(9), 1755–1758, doi:10.1029/2000GL012244.

Gnanadesikan, A. (1999), A simple predictive model for the structure of the oceanic pycnocline, *Science*, 283, 2077–2079, doi:10.1126/science.283.5410.2077.

Gnanadesikan, A., and R. W. Hallberg (2000), On the relationship of the Circumpolar Current to Southern Hemisphere winds in coarse-resolution ocean models, *J. Phys. Oceanogr.*, 30, 2013–2034, doi:10.1175/1520-0485(2000)030<2013:OTROTC>2.0.CO;2.

Gordon, A. L. (1967), Geostrophic transport through the Drake Passage, *Science*, 156, 1732–1734, doi:10.1126/science.156.3783.1732.

Gordon, A. L. (1986), Interocean exchange of thermocline water, *J. Geophys. Res.*, 91, 5037–5046, doi:10.1029/JC091iC04p05037.

Gordon, A. L., M. Visbeck, and B. Huber (2001), Export of Weddell Sea Deep and Bottom Water, *J. Geophys. Res.*, 106, 9005–9017, doi:10.1029/2000JC000281.

Gordon, A. L., B. Huber, D. McKee, and M. Visbeck (2010), A seasonal cycle in the export of bottom water from the Weddell Sea, *Nat. Geosci.*, 3, 551–556, doi:10.1038/ngeo916.

Hall, A., and M. Visbeck (2002), Synchronous variability in the Southern Hemisphere atmosphere, sea ice, and ocean resulting from the annular mode, *J. Clim.*, 15, 3043–3057, doi:10.1175/1520-0442(2002)015<3043:SVITSH>2.0.CO;2.

Hallberg, R., and A. Gnanadesikan (2006), The role of eddies in determining the structure and response of the wind-driven Southern Hemisphere overturning: Results from the Modeling Eddies in the Southern Ocean (MESO) project, *J. Phys. Oceanogr.*, 36, 2232–2252, doi:10.1175/JPO2980.1.

Hanawa, K., and L. D. Talley (2001), Mode waters, in *Ocean Circulation and Climate, Int. Geophys. Ser.*, vol. 77, edited by G. Siedler and J. Church, pp. 373–386, Academic, doi:10.1016/S0074-6142(01)80129-7.

Hewitt, R. P., D. A. Demer, and J. H. Emery (2003), An 8-year cycle in krill biomass density inferred from acoustic surveys conducted in the vicinity of the South Shetland Islands during the austral summers of 1991–1992 through 2001–2002, *Aquat. Living Resour.*, 16, 205–213, doi:10.1016/S0990-7440(03)00019-6.

Heywood, K. J., A. C. Naveira Garabato, and D. P. Stevens (2002), High mixing rates in the abyssal Southern Ocean, *Nature*, 415, 1011–1014, doi:10.1038/4151011a.

Heywood, K. J., J. L. Collins, C. W. Hughes, and J. M. Vassie (2007), On the detectability of internal tides in Drake Passage, *Deep Sea Res., Part I*, 54(11), 1972–1984, doi:10.1016/j.dsr.2007.08.002.

Hibbert, A., et al. (2010), Quasi-biennial modulation of the Southern Ocean coherent mode, *Q. J. R. Meteorol. Soc.*, 136, 755–768.

Hughes, C. W., and E. R. Ash (2001), Eddy forcing of the mean flow in the Southern Ocean, *J. Geophys. Res.*, 106, 2713–2722.

Hughes, C. W., and M. P. Meredith (2006), Coherent sea-level fluctuations along the global continental slope, *Philos. Trans. R. Soc. A*, *364*, 885–901, doi:10.1098/rsta.2006.1744.

Hughes, C. W., and V. Stepanov (2004), Ocean dynamics associated with rapid J2 fluctuations: Importance of circumpolar modes and identification of a coherent Arctic mode, *J. Geophys. Res.*, *109*, C06002, doi:10.1029/2003JC002176.

Hughes, C. W., M. P. Meredith, and K. J. Heywood (1999), Wind-forced transport fluctuations at Drake Passage: A southern mode, *J. Phys. Oceanogr.*, *29*(8), 1971–1992, doi:10.1175/1520-0485(1999)029<1971:WDTFTD>2.0.CO;2.

Hughes, C. W., P. L. Woodworth, M. P. Meredith, V. Stepanov, T. Whitworth III, and A. Pyne (2003), Coherence of Antarctic sea levels, Southern Hemisphere Annular Mode, and flow through Drake Passage, *Geophys. Res. Lett.*, *30*(9), 1464, doi:10.1029/2003GL017240.

Johnson, G. C., and H. Bryden (1989), On the strength of the Circumpolar Current, *Deep Sea Res., Part A*, *36*, 39–53, doi:10.1016/0198-0149(89)90017-4.

Johnson, G. C., and S. C. Doney (2006), Recent western South Atlantic bottom water warming, *Geophys. Res. Lett.*, *33*, L14614, doi:10.1029/2006GL026769.

Johnson, G. C., S. G. Purkey, and J. M. Toole (2008), Reduced Antarctic meridional overturning circulation reaches the North Atlantic Ocean, *Geophys. Res. Lett.*, *35*, L22601, doi:10.1029/2008GL035619.

Johnson, M. A. (1989), Forcing the volume transport through Drake Passage, *J. Geophys. Res.*, *94*, 16,115–16,124, doi:10.1029/JC094iC11p16115.

Jullion, L., S. C. Jones, A. C. Naveira Garabato, and M. P. Meredith (2010), Wind-controlled export of Antarctic Bottom Water from the Weddell Sea, *Geophys. Res. Lett.*, *37*, L09609, doi:10.1029/2010GL042822.

Karsten, R., H. Jones, and J. Marshall (2002), The role of eddy transfer in setting the stratification and transport of a circumpolar current, *J. Phys. Oceanogr.*, *32*, 39–54, doi:10.1175/1520-0485(2002)032<0039:TROETI>2.0.CO;2.

Karsten, R. H., and J. Marshall (2002), Constructing the residual circulation of the ACC from observations, *J. Phys. Oceanogr.*, *32*, 3315–3327, doi:10.1175/1520-0485(2002)032<3315:CTRCOT>2.0.CO;2.

King, B. A. (2001), Introduction to special section: World Ocean Circulation Experiment: Southern Ocean results, *J. Geophys. Res.*, *106*, 2691, doi:10.1029/2000JC900152.

Kusahara, K., and K. I. Ohshima (2009), Dynamics of the wind-driven sea level variations around Antarctica, *J. Phys. Oceanogr.*, *39*, 658–674, doi:10.1175/2008JPO3982.1.

Ledwell, J. R., L. C. St. Laurent, J. B. Girton, and J. M. Toole (2011), Diapycnal mixing in the Antarctic Circumpolar Current, *J. Phys. Oceanogr.*, *41*, 241–246, doi:10.1175/2010JPO4557.1.

Legeckis, R. (1977), Oceanic polar front in the Drake Passage — satellite observations during 1976, *Deep Sea Res.*, *24*, 701–704, doi:10.1016/0146-6291(77)90510-0.

Lenn, Y.-D., and T. K. Chereskin (2009), Observations of Ekman Currents in the Southern Ocean, *J. Phys. Oceanogr.*, *39*, 768–779, doi:10.1175/2008JPO3943.1.

Lenn, Y.-D., T. K. Chereskin, J. Sprintall, and E. Firing (2007), Mean jets, mesoscale variability and eddy momentum fluxes in the surface-layer of the Antarctic Circumpolar Current in Drake Passage, *J. Mar. Res.*, *65*, 27–58, doi:10.1357/002224007780388694.

Lenn, Y.-D., T. K. Chereskin, and J. Sprintall (2008), Improving estimates of the Antarctic Circumpolar Current streamlines in Drake Passage, *J. Phys. Oceanogr.*, *38*, 1000–1010, doi:10.1175/2007JPO3834.1.

Lenn, Y.-D., T. K. Chereskin, J. Sprintall, and J. L. McClean (2011), Near-surface eddy heat and momentum fluxes in the Antarctic Circumpolar Current in Drake Passage, *J. Phys. Oceanogr.*, *41*, 1385–1407, doi:10.1175/JPO-D-10-05017.1.

Livermore, R., A. Nankivell, G. Eagles, and P. Morris (2005), Paleogene opening of Drake Passage, *Earth Planet. Sci. Lett.*, *236*, 459–470, doi:10.1016/j.epsl.2005.03.027.

Loeb, V., V. Siegel, O. Holm-Hansen, R. Hewitt, W. Fraser, W. Trivelpiece, and S. Trivelpiece (1997), Effects of sea-ice extent and krill or salp dominance on the Antarctic food web, *Nature*, *387*, 897–900, doi:10.1038/43174.

Lumpkin, R., and K. Speer (2007), Global ocean meridional overturning, *J. Phys. Oceanogr.*, *37*, 2550–2562, doi:10.1175/JPO3130.1.

Mackintosh, N. A. (1934), Distribution of the macroplankton in the Atlantic sector of the Antarctic, in *Discovery Reports*, vol. 9, pp. 65–160, Cambridge Univ. Press, Cambridge, U. K.

Madden, R. A., and P. R. Julian (1971), Detection of a 40–50 day oscillation in the zonal wind in the tropical Pacific, *J. Atmos. Sci.*, *28*, 702–708, doi:10.1175/1520-0469(1971)028<0702:DOADOI>2.0.CO;2.

Marshall, D. P. (1997), Subduction of water masses in an eddying ocean, *J. Mar. Res.*, *55*, 201–222, doi:10.1357/0022240973224373.

Marshall, G. J. (2003), Trends in the Southern Annular Mode from observations and reanalyses, *J. Clim.*, *16*, 4134–4143, doi:10.1175/1520-0442(2003)016<4134:TITSAM>2.0.CO;2.

Marshall, J., and T. Radko (2003), Residual-mean solutions for the Antarctic Circumpolar Current and its associated overturning circulation, *J. Phys. Oceanogr.*, *33*, 2341–2354, doi:10.1175/1520-0485(2003)033<2341:RSFTAC>2.0.CO;2.

Marshall, J., and T. Radko (2006), A model of the upper branch of the meridional overturning circulation of the Southern Ocean, *Prog. Oceanogr.*, *70*, 331–345, doi:10.1016/j.pocean.2006.07.004.

Marshall, J., E. Shuckburgh, H. Jones, and C. Hill (2006), Estimates and implications of surface eddy diffusivity in the Southern Ocean derived from tracer transport, *J. Phys. Oceanogr.*, *36*, 1806–1821, doi:10.1175/JPO2949.1.

Matthews, A. J., and M. P. Meredith (2004), Variability of the Antarctic circumpolar transport and the Southern Annular Mode associated with the Madden-Julian Oscillation, *Geophys. Res. Lett.*, *31*, L24312, doi:10.1029/2004GL021666.

Maximenko, N., and P. P. Niiler (2005), Hybrid decade-mean global sea level with mesoscale resolution, in *Recent Advances in Marine Science and Technology*, edited by N. Saxena, pp. 55–59, PACON Int., Honolulu, Hawaii.

Mazloff, M. R., P. Heimbach, and C. Wunsch (2010), An eddy permitting Southern Ocean state estimate, *J. Phys. Oceanogr.*, *40*, 880–899, doi:10.1175/2009JPO4236.1.

Meinen, C. S., D. S. Luther, and D. R. Watts (2003), Mean stream coordinates structure of the Subantarctic Front: Temperature, salinity and absolute velocity, *J. Geophys. Res.*, *108*(C8), 3263, doi:10.1029/2002JC001545.

Meredith, M. P., and A. M. Hogg (2006), Circumpolar response of Southern Ocean eddy activity to a change in the Southern Annular Mode, *Geophys. Res. Lett.*, *33*, L16608, doi:10.1029/2006GL026499.

Meredith, M. P., and C. W. Hughes (2005), On the sampling time scale required to reliably monitor interannual variability in the Antarctic circumpolar transport, *Geophys. Res. Lett.*, *32*, L03609, doi:10.1029/2004GL022086.

Meredith, M. P., and J. C. King (2005), Rapid climate change in the ocean to the west of the Antarctic Peninsula during the second half of the twentieth century, *Geophys. Res. Lett.*, *32*, L19604, doi:10.1029/2005GL024042.

Meredith, M. P., J. M. Vassie, K. J. Heywood, and R. Spencer (1996), On the temporal variability of the transport through Drake Passage, *J. Geophys. Res.*, *101*, 22,485–22,494, doi:10.1029/96JC02003.

Meredith, M. P., J. M. Vassie, R. Spencer, and K. J. Heywood (1997), The processing and application of inverted echo sounder data from Drake Passage, *J. Atmos. Oceanic Technol.*, *14*(4),

871–882, doi:10.1175/1520-0426(1997)014<0871:TPAAOI>2.0. CO;2.

Meredith, M. P., C. W. Hughes, and P. R. Foden (2003), Down-slope convection north of Elephant Island, Antarctic Peninsula: Influence on deep waters and dependence on ENSO, *Geophys. Res. Lett.*, *30*(9), 1462, doi:10.1029/2003GL017074.

Meredith, M. P., P. L. Woodworth, C. W. Hughes, and V. Stepanov (2004), Changes in the ocean transport through Drake Passage during the 1980s and 1990s, forced by changes in the Southern Annular Mode, *Geophys. Res. Lett.*, *31*, L21305, doi:10.1029/2004GL021169.

Meredith, M. P., A. C. Naveira Garabato, A. L. Gordon, and G. C. Johnson (2008), Evolution of the deep and bottom waters of the Scotia Sea, Southern Ocean, 1995–2005, *J. Clim.*, *21*(13), 3327–3343, doi:10.1175/2007JCLI2238.1.

Meredith, M. P., A. L. Gordon, A. C. Naveira Garabato, E. P. Abrahamsen, B. A. Huber, L. Jullion, and H. J. Venables (2011), Synchronous intensification and warming of Antarctic Bottom Water outflow from the Weddell Gyre, *Geophys. Res. Lett.*, *38*, L03603, doi:10.1029/2010GL046265.

Mignone, B. K., A. Gnanadesikan, J. L. Sarmiento, and R. D. Slater (2006), Central role of Southern Hemisphere winds and eddies in modulating the oceanic uptake of anthropogenic carbon, *Geophys. Res. Lett.*, *33*, L01604, doi:10.1029/2005GL024464.

Morrow, R. A., R. Coleman, J. A. Church, and D. B. Chelton (1994), Surface eddy momentum flux and velocity variances in the Southern Ocean from Geosat altimetry, *J. Phys. Oceanogr.*, *24*, 2050–2071, doi:10.1175/1520-0485(1994)024<2050:SEMFAV>2.0.CO;2.

Munday, D. R., L. C. Allison, H. L. Johnson, and D. P. Marshall (2011), Remote forcing of the Antarctic Circumpolar Current by diapycnal mixing, *Geophys. Res. Lett.*, *38*, L08609, doi:10.1029/2011GL046849.

Munk, W. H., and E. Palmén (1951), Note on the dynamics of the Antarctic Circumpolar Current, *Tellus*, *3*, 53–55, doi:10.1111/j.2153-3490.1951.tb00776.x.

Naveira Garabato, A. C., K. J. Heywood, and D. P. Stevens (2002a), Modification and pathways of Southern Ocean deep waters in the Scotia Sea, *Deep Sea Res., Part I*, *49*, 681–705, doi:10.1016/S0967-0637(01)00071-1.

Naveira Garabato, A. C., E. L. McDonagh, D. P. Stevens, K. J. Heywood, and R. J. Sanders (2002b), On the export of Antarctic Bottom Water from the Weddell Sea, *Deep Sea Res., Part II*, *49*, 4715–4742, doi:10.1016/S0967-0645(02)00156-X.

Naveira Garabato, A. C., K. L. Polzin, B. A. King, K. J. Heywood, and M. Visbeck (2004), Widespread intense turbulent mixing in the Southern Ocean, *Science*, *303*, 210–213, doi:10.1126/science.1090929.

Naveira Garabato, A. C., D. P. Stevens, A. J. Watson, and W. Roether (2007), Short-circuiting of the overturning circulation of the Antarctic Circumpolar Current, *Nature*, *447*, 194–197, doi:10.1038/nature05832.

Naveira Garabato, A. C., L. Jullion, D. P. Stevens, K. J. Heywood, and B. A. King (2009), Variability of Subantarctic Mode Water and Antarctic Intermediate Water in Drake Passage during the late 20th and early 21st centuries, *J. Clim.*, *22*(13), 3661–3688, doi:10.1175/2009JCLI2621.1.

Naveira Garabato, A. C., R. Ferrari, and K. L. Polzin (2011), Eddy stirring in the Southern Ocean, *J. Geophys. Res.*, *116*, C09019, doi:10.1029/2010JC006818.

Nikurashin, M., and R. Ferrari (2010), Radiation and dissipation of internal waves generated by geostrophic motions impinging on small-scale topography: Application to the Southern Ocean, *J. Phys. Oceanogr.*, *40*, 2025–2042, doi:10.1175/2010JPO4315.1.

Nowlin, W. D., and M. Clifford (1982), The kinematic and thermohaline zonation of the Antarctic Circumpolar Current at Drake Passage, *J. Mar. Res.*, *40*, 481–507.

Nowlin, W. D., T. Whitworth III, and R. D. Pillsbury (1977), Structure and transport of the Antarctic Circumpolar Current at

Drake Passage from short-term measurements, *J. Phys. Oceanogr.*, *7*, 788–802, doi:10.1175/1520-0485(1977)007<0788:SATOTA>2.0.CO;2.

Oke, P. R., and M. H. England (2004), Oceanic response to changes in the latitude of the Southern Hemisphere subpolar westerly winds, *J. Clim.*, *17*, 1040–1054, doi:10.1175/1520-0442(2004)017<1040:ORTCIT>2.0.CO;2.

Olbers, D. (1998), Comments on "On the obscurantist physics of 'form drag' in theorizing about the Antarctic Circumpolar Current," *J. Phys. Oceanogr.*, *28*, 1647–1654, doi:10.1175/1520-0485(1998)028<1647:COOTOP>2.0.CO;2.

Olbers, D., and K. Lettmann (2007), Barotropic and baroclinic processes in the transport variability of the Antarctic Circumpolar Current, *Ocean Dyn.*, *57*, 559–578, doi:10.1007/s10236-007-0126-1.

Olbers, D., and M. Visbeck (2005), A model of the zonally averaged stratification and overturning in the Southern Ocean, *J. Phys. Oceanogr.*, *35*, 1190–1205, doi:10.1175/JPO2750.1.

Olbers, D., V. Gouretski, G. Seiss, and J. Schröter (1992), *Hydrographic Atlas of the Southern Ocean*, Alfred-Wegener Inst., Bremerhave, Germany.

Orsi, A. H., T. Whitworth III, and W. D. Nowlin (1995), On the meridional extent and fronts of the Antarctic Circumpolar Current, *Deep Sea Res., Part I*, *42*(5), 641–673, doi:10.1016/0967-0637(95)00021-W.

Orsi, A. H., G. C. Johnson, and J. L. Bullister (1999), Circulation, mixing, and production of Antarctic Bottom Water, *Prog. Oceanogr.*, *43*(1), 55–109, doi:10.1016/S0079-6611(99)00004-X.

Ostapoff, F. (1961), A contribution to the problem of the Drake Passage transport, *Deep Sea Res.*, *8*, 111–120, doi:10.1016/0146-6313(61)90003-X.

Peterson, R. G. (1988a), On the transport of the Antarctic Circumpolar Current through Drake Passage and its relation to wind, *J. Geophys. Res.*, *93*, 13,993–14,004, doi:10.1029/JC093iC11p13993.

Peterson, R. G. (1988b), Comparisons of sea level and bottom pressure measurements at Drake Passage, *J. Geophys. Res.*, *93*, 12,439–12,448, doi:10.1029/JC093iC10p12439.

Phillips, H. E., and S. R. Rintoul (2000), Eddy variability and energetics from direct current measurements in the Antarctic Circumpolar Current south of Australia, *J. Phys. Oceanogr.*, *30*, 3050–3076, doi:10.1175/1520-0485(2000)030<3050:EVAEFD>2.0.CO;2.

Ponte, R. M., and K. J. Quinn (2009), Bottom pressure changes around Antarctica and wind-driven meridional flows, *Geophys. Res. Lett.*, *36*, L13604, doi:10.1029/2009GL039060.

Provost, C., A. Renault, N. Barré, N. Sennechael, V. Garcon, J. Sudre, and O. Huhn (2011), Two repeat crossings of Drake Passage in austral summer 2006: Short term variations and evidence for considerable ventilation of intermediate and deep waters, *Deep Sea Res., Part II*, *58*, 2555–2571, doi:10.1016/j.dsr2.2011.06.009.

Rabinovich, A. B., P. L. Woodworth, and V. V. Titov (2011), Deep-sea observations and modeling of the 2004 Sumatra tsunami in Drake Passage, *Geophys. Res. Lett.*, *38*, L16604, doi:10.1029/2011GL048305.

Reid, J. L., and W. D. Nowlin (1971), Transport of water through the Drake Passage, *Deep Sea Res. Oceanogr. Abstr.*, *18*, 51–64.

Renault, A., C. Provost, N. Sennechael, N. Barré, and A. Kartavtseff (2011), Two full-depth velocity surveys in the Drake Passage in 2006: Transport estimates, *Deep Sea Res., Part II*, *58*, 2572–2591, doi:10.1016/j.dsr2.2011.01.004.

Rintoul, S. R., C. Hughes, and D. Olbers (2001), The Antarctic Circumpolar Current system, in *Ocean Circulation and Climate*, edited by G. Sielder et al., pp. 271–302, Academic, San Diego, Calif., doi:10.1016/S0074-6142(01)80124-8.

Rintoul, S. R., M. Sparrow, M. P. Meredith, V. Wadley, K. Speer, E. Hofmann, C. Summerhayes, E. Urban, and R. Bellerby (2010), Southern Ocean Observing System (SOOS): Rationale and strategy for sustained observations of the Southern Ocean,

in *Proceedings of OceanObs '09: Sustained Ocean Observations and Information for Society*, edited by J. Hall, D. E. Harrison, and D. Stammer, 12 pp., *Eur. Space Agency*, doi:10.5270/OceanObs09.cwp.74.

Robertson, R., M. Visbeck, A. L. Gordon, and E. Fahrbach (2002), Long-term temperature trends in the deep waters of the Weddell Sea, *Deep Sea Res., Part II*, 49, 4791–4806, doi:10.1016/S0967-0645(02)00159-5.

Roscoe, H. K., and J. D. Haigh (2007), Influences of ozone depletion, the solar cycle and the QBO on the Southern Annular Mode, *Q. J. R. Meteorol. Soc.*, 133, 1855–1864, doi:10.1002/qj.153.

Sabine, C. L., et al. (2004), The oceanic sink for anthropogenic CO_2, *Science*, 305, 367–371, doi:10.1126/science.1097403.

Sallée, J. B., K. Speer, S. R. Rintoul, and S. Wijffels (2010), Southern Ocean thermocline ventilation, *J. Phys. Oceanogr.*, 40, 509–529, doi:10.1175/2009JPO4291.1.

Scher, H. D., and E. E. Martin (2006), Timing and climatic consequences of the opening of Drake Passage, *Science*, 312, 428–430, doi:10.1126/science.1120044.

Schofield, O., H. W. Ducklow, D. G. Martinson, M. P. Meredith, M. A. Moline, and W. R. Fraser (2010), How do polar marine ecosystems respond to rapid climate change?, *Science*, 328, 1520–1523.

Sciremammano, F. (1979), Observations of Antarctic Polar Front motions in a deep water expression, *J. Phys. Oceanogr.*, 9, 221–226, doi:10.1175/1520-0485(1979)009<0221:OOAPFM>2.0.CO;2.

Siedler, G., J. Church, and W. J. Gould (2001), *Ocean Circulation and Climate: Observing and Modeling the Global Ocean*, *Int. Geophys. Ser.*, vol. 77, 715 pp., Academic, San Diego, Calif.

Sloyan, B. M., and S. R. Rintoul (2001), The Southern Ocean limb of the global deep overturning circulation, *J. Phys. Oceanogr.*, 31, 143–173, doi:10.1175/1520-0485(2001)031<0143:TSOLOT>2.0.CO;2.

Smith, K. S., and J. Marshall (2009), Evidence for enhanced eddy mixing at mid-depth in the Southern Ocean, *J. Phys. Oceanogr.*, 39, 50–69, doi:10.1175/2008JPO3880.1.

Sokolov, S., and S. R. Rintoul (2007), Multiple jets of the Antarctic Circumpolar Current south of Australia, *J. Phys. Oceanogr.*, 37, 1394–1412, doi:10.1175/JPO3111.1.

Speer, K., S. R. Rintoul, and B. Sloyan (2000), The diabatic Deacon cell, *J. Phys. Oceanogr.*, 30, 3212–3222, doi:10.1175/1520-0485(2000)030<3212:TDDC>2.0.CO;2.

Spencer, R., and P. R. Foden (1996), Data from the deep ocean via releasable data capsules, *Sea Technol.*, 37(2), 10–12.

Sprintall, J. (2003), Seasonal to interannual upper-ocean variability in the Drake Passage, *J. Mar. Res.*, 61, 27–57, doi:10.1357/002224003321586408.

Sprintall, J. (2008), Long-term trends and interannual variability of temperature in Drake Passage, *Prog. Oceanogr.*, 77, 316–330, doi:10.1016/j.pocean.2006.06.004.

Straub, D. N. (1993), On the transport and angular momentum balance of channel models of the Antarctic Circumpolar Current, *J. Phys. Oceanogr.*, 23, 776–782, doi:10.1175/1520-0485(1993)023<0776:OTTAAM>2.0.CO;2.

Sudre, J., V. Garcon, C. Provost, N. Sennechael, O. Huhn, and M. Lacombe (2011), Short-term variations of deep water masses in Drake Passage revealed by a multiparametric analysis of the ANT-XXIII/3 bottle data, *Deep Sea Res., Part II*, 58, 2592–2612, doi:10.1016/j.dsr2.2011.01.005.

Talley, L. D. (2008), Freshwater transport estimates and the global overturning circulation: Shallow, deep and throughflow components, *Prog. Oceanogr.*, 78, 257–303, doi:10.1016/j.pocean.2008.05.001.

Talley, L. D., J. L. Reid, and P. E. Robbins (2003), Data-based meridional overturning streamfunctions for the global ocean, *J. Clim.*, 16, 3213–3226, doi:10.1175/1520-0442(2003)016<3213:DMOSFT>2.0.CO;2.

Thompson, A. F., S. T. Gille, J. MacKinnon, and J. Sprintall (2007), Spatial and temporal scales of small-scale mixing in Drake Passage, *J. Phys. Oceanogr.*, 37, 572–592, doi:10.1175/JPO3021.1.

Thompson, D. W. J., and S. Solomon (2002), Interpretation of recent Southern Hemisphere climate change, *Science*, 296, 895–899, doi:10.1126/science.1069270.

Thompson, D. W. J., and J. M. Wallace (2000), Annular modes in the extratropical circulation. Part I: Month-to-month variability, *J. Clim.*, 13, 1000–1016, doi:10.1175/1520-0442(2000)013<1000:AMITEC>2.0.CO;2.

Thompson, D. W. J., J. M. Wallace, and G. C. Hegerl (2000), Annular modes in the extratropical circulation. Part II: Trends, *J. Clim.*, 13, 1018–1036, doi:10.1175/1520-0442(2000)013<1018:AMITEC>2.0.CO;2.

Toggweiler, J. R., and B. Samuels (1995), Effect of Drake Passage on the global thermohaline circulation, *Deep Sea Res., Part I*, 42, 477–500, doi:10.1016/0967-0637(95)00012-U.

Tokmakian, R., and P. G. Challenor (1999), On the joint estimation of model and satellite sea surface height anomaly errors, *Ocean Modell.*, 1, 39–52, doi:10.1016/S1463-5003(99)00006-2.

Vallis, G. K. (2000), Large-scale circulation and production of stratification: Effects of wind, geometry and diffusion, *J. Phys. Oceanogr.*, 30, 933–954, doi:10.1175/1520-0485(2000)030<0933:LSCAPO>2.0.CO;2.

Vaughan, D. G., G. J. Marshall, W. M. Connolley, C. Parkinson, R. Mulvaney, D. A. Hodgson, J. C. King, C. J. Pudsey, and J. Turner (2003), Recent rapid regional climate warming on the Antarctic Peninsula, *Clim. Change*, 60(3), 243–274, doi:10.1023/A:1026021217991.

Visbeck, M. (2009), A station-based Southern Annular Mode index from 1884 to 2005, *J. Clim.*, 22, 940–950, doi:10.1175/2008JCLI2260.1.

Vivier, F., and C. Provost (1999), Volume transport of the Malvinas Current: Can the flow be monitored by TOPEX/Poseidon?, *J. Geophys. Res.*, 104, 21,105–21,122, doi:10.1029/1999JC900056.

Vivier, F., C. Provost, and M. P. Meredith (2001), Remote and local forcing in the Brazil-Malvinas Region, *J. Phys. Oceanogr.*, 31, 892–913, doi:10.1175/1520-0485(2001)031<0892:RALFIT>2.0.CO;2.

Vivier, F., K. A. Kelly, and M. Harismendy (2005), Causes of large-scale sea level variations in the Southern Ocean: Analyses of sea level and a barotropic model, *J. Geophys. Res.*, 110, C09014, doi:10.1029/2004JC002773.

Watson, A. J., and A. C. Naveira Garabato (2006), The role of Southern Ocean mixing and upwelling in glacial-interglacial atmospheric CO_2 change, *Tellus Ser. B*, 58, 73–87.

Watts, D. R., C. Sun, and S. Rintoul (2001), A two-dimensional gravest empirical mode determined from hydrographic observations in the Subantarctic Front, *J. Phys. Oceanogr.*, 31, 2186–2209, doi:10.1175/1520-0485(2001)031<2186:ATDGEM>2.0.CO;2.

Wearn, R. B., and D. J. Baker (1980), Bottom pressure measurements across the Antarctic Circumpolar Current and their relation to the wind, *Deep Sea Res., Part A*, 27, 875–888, doi:10.1016/0198-0149(80)90001-1.

Webb, D. J. (1998), The first main run of the OCCAM global ocean model, internal document, Southampton Oceanogr. Centre, Southhampton, U. K.

Weijer, W., and S. T. Gille (2005), Adjustment of the Southern Ocean to wind forcing on synoptic time scales, *J. Phys. Oceanogr.*, 35, 2076–2089, doi:10.1175/JPO2801.1.

Whitworth, T. (1980), Zonation and geostrophic flow of the Antarctic Circumpolar Current at Drake Passage, *Deep Sea Res., Part A*, 27, 497–507, doi:10.1016/0198-0149(80)90036-9.

Whitworth, T. (1983), Monitoring the transport of the Antarctic Circumpolar Current at Drake Passage, *J. Phys. Oceanogr.*, 13, 2045–2057, doi:10.1175/1520-0485(1983)013<2045:MTTOTA>2.0.CO;2.

Whitworth, T., and R. G. Peterson (1985), Volume transport of the Antarctic Circumpolar Current from bottom pressure measure-

ments, *J. Phys. Oceanogr.*, *15*, 810–816, doi:10.1175/1520-0485 (1985)015<0810:VTOTAC>2.0.CO;2.

Wong, S., and W. Wang (2003), Tropical-extratropical connection in interannual variation of the tropopause: Comparison between NCEP/NCAR reanalysis and an atmospheric general circulation model simulation, *J. Geophys. Res.*, *108*(D2), 4043, doi:10.1029/2001JD002016.

Woodworth, P. L., J. M. Vassie, C. W. Hughes, and M. P. Meredith (1996), A test of the ability of TOPEX/POSEIDON to monitor flows through the Drake Passage, *J. Geophys. Res.*, *101*, 11,935–11,947, doi:10.1029/96JC00350.

Woodworth, P. L., D. T. Pugh, M. P. Meredith, and D. L. Blackman (2005), Sea level changes at Port Stanley, Falkland Islands, *J. Geophys. Res.*, *110*, C06013, doi:10.1029/2004JC002648.

Wunsch, C., and R. Ferrari (2004), Vertical mixing, energy, and the general circulation of the oceans, *Annu. Rev. Fluid Mech.*, *36*, 281–314, doi:10.1146/annurev.fluid.36.050802.122121.

Xie, P., and P. A. Arkin (1997), Global Precipitation: A 17-year monthly analysis based on gauge observations, satellite estimates and numerical model outputs, *Bull. Am. Meteorol. Soc.*, *78*, 2539–2558, doi:10.1175/1520-0477(1997)078<2539:GPAYMA>2.0.CO;2.

Zachos, J., M. Pagani, L. Sloan, E. Thomas, and K. Billups (2001), Trends, rhythms and aberrations in global climate 65 Ma to present, *Science*, *292*, 686–693, doi:10.1126/science.1059412.

Zhou, M., W. Nordhausen, and M. Huntley (1994), ADCP measurements of the distribution and abundance of euphausiids near the Antarctic Peninsula in winter, *Deep Sea Res., Part I*, *41*, 1425–1445, doi:10.1016/0967-0637(94)90106-6.

Zika, J. D., B. M. Sloyan, and T. J. McDougall (2009), Diagnosing the Southern Ocean overturning from tracer fields, *J. Phys. Oceanogr.*, *39*, 2926–2940, doi:10.1175/2009JPO4052.1.

L. C. Allison, Department of Meteorology, University of Reading, Earley Gate, Reading RG6 6BB, UK.

G. R. Bigg, Department of Geography, University of Sheffield, Winter Street, Sheffield S10 2TN, UK.

T. K. Chereskin and J. Sprintall, Scripps Institution of Oceanography, 9500 Gilman Dr., La Jolla, CA 92093-0230, USA.

K. Donohue, Graduate School of Oceanography, University of Rhode Island, 215 S. Ferry Rd., Kingston, RI 02882, USA.

K. J. Heywood, School of Environmental Sciences, University of East Anglia, Norwich NR4 7TJ, UK.

A. Hibbert and H. Leach, Department of Earth and Ocean Sciences, University of Liverpool, 4 Brownlow St., Liverpool L69 3GP, UK.

C. W. Hughes, M. A. Morales Maqueda, and P. L. Woodworth, National Oceanography Centre, 6 Brownlow St., Liverpool L3 5DA, UK.

H. L. Johnson, Department of Earth Sciences, University of Oxford, South Parks Road, Oxford OX1 3AN, UK.

L. Jullion, B. A. King, and A. C. Naveira Garabato, National Oceanography Centre, Southampton SO14 3ZH, UK.

Y.-D. Lenn, School of Ocean Sciences, Bangor University, Bangor LL59 5AB, UK.

D. P. Marshall and D. R. Munday, Atmospheric, Oceanic and Planetary Physics, University of Oxford, Parks Road, Oxford OX1 3PU, UK.

A. McC. Hogg, Research School of Earth Sciences, Australian National University, Canberra, ACT 0200, Australia.

M. P. Meredith and J.-B. Sallée, British Antarctic Survey, Madingley Road, Cambridge CB3 0ET, UK. (mmm@bas.ac.uk)

C. Provost, LOCEAN, Université Pierre et Marie Curie, 4 Pl. Jussieu, Paris F-75252, France.